12-2007

Adipocyte Response To Injectable Beads Engineered For Breast Tissue Reconstruction

Katherine Neser
Clemson University, kneser@gmail.com

ADIPOCYTE RESPONSE TO INJECTABLE BEADS ENGINEERED FOR BREAST TISSUE RECONSTRUCTION

A Thesis
Presented to
the Graduate School of
Clemson University

In Partial Fulfillment
of the Requirements for the Degree
Master of Science
Bioengineering

---

by
Katherine Anne Neser
December 2007

Accepted by:
Karen J. L. Burg, Ph.D., Committee Chair
Martine LaBerge, Ph.D.
Susan Duckett, Ph.D.

ABSTRACT

It is estimated that over 150,000 patients will be diagnosed with invasive breast cancer in 2007. Patients must undergo a mastectomy or a lumpectomy to remove the cancerous tissue, but only a mastectomy allows breast reconstructive surgery. Due to the limitations of current reconstruction options, new alternatives are being explored. Injectable materials have been suggested for breast tissue reconstruction because of their versatility. Cells cultured on injectable beads form cell carriers that may be mixed with a hydrogel, resulting in a construct that may be injected through a syringe to restore normal tissue mass. This solution offers breast cancer patients a new reconstructive option that employs their own healthy cells.

The long-term objective, beyond the scope of this research, is to develop a novel injectable composite system, consisting of cellular scaffolds in a hydrogel carrier that could be injected into a defect site. The primary goal of this research was to develop viable polymer scaffolds for preadipocyte growth and differentiation and to assess the cellular response to these scaffolds. Initially, collagen-polylactide beads were developed and seeded with fibroblasts. The fibroblasts had a high affinity for these beads, but collagen was not conclusively proven to be present in the microspheres. Subsequently, polylactide beads with collagen or collagen and linoleic acid coatings were produced. Preadipocytes were grown on the collagen and collagen/linoleic acid coated beads, uncoated polylactide beads, or two 2-D controls, and tested for viability, lipid and fatty acid production, and gene expression. Few cells were capable of attaching and proliferating on the uncoated polylactide beads for the entire 18-Day culture period;

however, more cells were able to attach and proliferate on both types of coated microcarriers. Cell produced more triglyceride on Day 18 of culture on the beads coated with collagen than the polylactide beads or the polylactide beads coated with collagen and linoleic acid. Cells grown on both types of coated beads produced more fatty acids on Day 18 than cells grown on the polylactide beads. The coated beads show potential for use in the injectable composite system as cellular carriers; however, the polylactide beads may be better suited for an alternative purpose in this system. Future work is needed to optimize the linoleic acid concentration as well as to examine other fatty acids for their effectiveness in inducing differentiation of preadipocytes.

DEDICATION

I dedicate this work to my family, whose support, encouragement, and love have made it possible for me to complete this work. Their inspiration and contributions along the way have helped me to finish this Master's degree and will continue to help me with all that I will accomplish in life.

ACKNOWLEDGMENTS

I would like to thank my advisor, Dr. Karen J. L. Burg for all of her guidance, support and encouragement. Her confidence in my abilities has provided motivation during the completion of this research and thesis. I would also like to thank my committee members, Dr. Susan Duckett and Dr. Martine LaBerge and for all of their time and assistance during the course of this research and completion of this thesis.

I would like to thank Kim Ivey for her technical assistance with the gel permeation chromatography and the Fourier transform infrared spectroscopy and Dr. Larry Grimes for his help with statistical analysis and statistical software programming. I am thankful for all my lab mates for their help, encouragement, and friendships, especially Cheryl Parzel and Cheryl Gomillion who lent so much time to help me with this work. Funding for this research was provided by the National Science Foundation: Presidential Early Career Award for Scientists and Engineers and the Department of Defense: Era of Hope Scholars Award

TABLE OF CONTENTS

Page

LIST OF TABLES

LIST OF FIGURES

PREFACE

Current methods of reconstructing breast tissue after a mastectomy or lumpectomy are limited, so new methods are being researched. Of particular interest is tissue engineering a minimally invasive device, such as an injectable biomaterial, to restore the breast tissue without the need for a second surgery. This method will reduce the pain, scarring, recovery time, and cost that usually occur with reconstructive surgery. Scaffolds for use in injectable devices are being designed and researched for their ability to control cellular activity, encourage tissue growth, and provide a temporary filler until the devices can be replaced by native tissue.

The purpose of this research was to add collagen and linoleic acid to polylactide microspheres and evaluate the cellular response to such microspheres. Two studies were conducted. First, collagen-polylactide beads were manufactured and tested for their cellular affinity. Second, polylactide beads were coated with collagen or with collagen and linoleic acid. Cells on both types of coated beads were tested for cell viability, triglyceride and fatty acid production, and gene expression, and the results were compared to those derived from cellular polylactide beads as well as 2-D surfaces.

INTRODUCTION

Breast cancer is the second most common cancer among women, second only to nonmelanoma skin cancers. The American Cancer Society estimates that 178,000 new cases of invasive breast cancer will occur in women in the US during 2007 [1]. Several potential courses of treatment are considered for these patients. Surgery and therapeutic options, such as radiation therapy, chemotherapy, and hormone therapy, are considered to be the standard treatments to remove a tumor. Most patients with breast cancer have surgery to remove the cancerous tissue; the two most common surgeries are lumpectomy and mastectomy. A lumpectomy is a breast conserving surgery, which removes the tumor and a small margin of normal tissue around it, but for which there are no reconstructive options available. A mastectomy removes the entire breast that contains cancer, and allows the patient to undergo breast reconstruction.

Breast Tissue Biology

Adipose tissue comprises most of the normal breast and is removed during mastectomy. This tissue is highly vascularized and has an extensive vascular network. The volume of an adipocyte is 80 to 95% triglyceride, which is a type of lipid. Mature adipocytes are terminally differentiated and cannot proliferate, but can increase in size. Preadipocytes have been investigated for adipose tissue engineering because these cells are committed to the adipocyte lineage and can increase in number [2]. Preadipocytes can be advantageous because of their proliferative capacity and ability to differentiate and form adipose tissue. *In vitro,* preadipocytes are fibroblast-like in appearance and this

shape is maintained throughout cellular proliferation. When preadipocytes undergo differentiation, proliferation is halted and the cells undergo morphological and biochemical changes [2]. The maturing cells acquire a spherical shape, accumulate triglyceride, and exhibit mature adipocyte phenotypes.

During the differentiation process, preadipocytes begin to express genes that are characteristic of adipocytes. Preadipocytes express the gene growth arrest and DNA-damage inducible protein (GADD) 153, also designated C/EBP-homologous protein zeta, (CHOP-10), which blocks the cell from transitioning from the G1 to the S phase of the cell cycle [3]. This gene inhibits adipocyte differentiation, and is down regulated as differentiation begins [3, 4]. Early in the differentiation stages peroxisome proliferator activator receptor gamma, PPAR-γ, is expressed and levels increase as differentiation progresses to later stages [2, 4]. PPAR-γ is a nuclear hormone receptor [4, 5, 6] that promotes and regulates adipogenesis [5, 7, 8]. Adipocyte-specific fatty-acid-binding protein-2 (aP-2) is a lipid binding protein [9] expressed in mature adipocytes [4, 6, 8].

Traditional Methods of Breast Reconstruction

According to the American Society for Plastic Surgeons, over 50,000 women opted for reconstructive surgery in 2006 [10]. The goals of reconstruction are to regain breast contour and chest symmetry, and to help women avoid the feeling of having a deformity. Reconstruction options include acellular and cellular approaches, which have their associated complications and disadvantages.

Acellular options include prostheses, tissue expanders, and implants that are all available commercially. Prostheses are worn outside the body and give a natural appearance when worn under clothing; prostheses lend a non-surgical option. These devices are mobile and therefore limit the patient's physical activity; additionally, prostheses may appear distorted at times. A tissue expander necessitates a surgical procedure where an empty silicone shell is placed under the muscle wall. The shell is filled with saline over a period of weeks to months until it is inflated to the proper size. The shell is then deflated and removed; the void is filled with a permanent implant. Risk of infection, damage to the expander, discomfort of expansion, a second operation, and a longer period of reconstruction are all potential negative outcomes following tissue expansion and reconstruction [11, 12]. Breast implants are silicone shells filled with either silicone or saline that may be implanted during or after the initial surgery. Common complications include rupture and subsequent removal of the implant. Scar tissue may contract and form a hard capsule around the implant, in rare cases masking the recurrence of breast tumors.

Cellular reconstructive options were initiated with the investigation of autologous adipose tissue for soft tissue repair. Adipose tissue is found in abundance in many patients, and is easily harvested [12]. However, when implanted, an adipose tissue graft volume decreases by 50-70% due to resorption of the tissue [12]. Adipocytes are anchorage-dependent cells and will not survive without a scaffold on which to grow. Mature adipocytes cannot grow to replenish the cells lost to resorption because they are terminally differentiated [12]. A tissue flap is a section of autologous tissue consisting of

skin, fat and/or muscle that is transplanted to the breast area [12]. The flap can be shaped to approximate the size and feel of a normal breast [13]. There are two main types of flaps; a TRAM flap and a Latissimus flap. The TRAM (transverse rectus abdominus musculocutaneous) flap is the most commonly excised flap. The abdominal wall skin, rectus abdominus muscle, and subcutaneous adipose tissue, along with the blood vessels that supply these tissues are moved to the chest to recreate the breast mound [12]. The Latissimus flap, including the latissimus dorsi muscle of the back, along with the skin and fat in the area, is moved to recreate the breast mound. This type of reconstruction minimizes foreign body response, and the reconstructed site more closely approximates the feel of a normal breast as opposed to an inert implant [13]. Donor-site morbidity, abdominal wall weakness or latissimus dorsi muscle atrophy at the donor site, and longer recovery times are the primary drawbacks of this surgery. These reconstruction options restore tissue volume, but do not restore tissue function or create a viable tissue mass.

Tissue Engineering as a Method of Breast Reconstruction

Tissue engineering strategies are being investigated for breast tissue reconstruction. This multidisciplinary field focuses the application of engineering and life science concepts toward the development of biological substitutes that restore, maintain, or improve tissue function [14]. Ideally, the engineered tissue integrates with the host tissue and new native tissue is created. The goal of breast tissue engineering is to create a volume of viable adipose tissue using the patient's cells as the building blocks. Direct autologous fat tissue transplantation is minimally successful because a significant

portion of the transplanted tissue resorbs over time leading to visible deformities [15]. Current tissue engineering strategies include scaffold guided tissue regeneration (e.g., injectable composite system), tissue based regeneration (e.g., fragmented omentum), and tissue induced regeneration (e.g., *de novo* adipogenesis) [15].

Breast Tissue Engineering Scaffolds

Scaffolds employed in adipose tissue engineering need to meet certain criteria. The scaffold should facilitate the growth of tissue that has the natural feel of the normal tissue and should conform to the defect site in the original tissue [16, 17]. A viable scaffold should be biocompatible, facilitate cell adhesion, promote cell growth, and act as a guide for the three-dimensional growth of cells [16, 17]. The scaffold porosity should be sufficient for cell adhesion and tissue ingrowth; the scaffold should have a large surface to volume ratio and should be eliminated completely and replaced by native tissue over a period of time [16, 17, 18]. The scaffold should degrade at a rate that allows the timely development of new tissue formation. Absorbable scaffolds are advantageous because they eliminate the need for a retrieval surgery and their absorption minimizes the possibility for long-term biocompatibility issues.

Preadipocytes and adipocytes are anchorage-dependent cells; i.e. they require a biomechanically acceptable substrate in order for normal cell proliferation and differentiation to occur [19]. Scaffolds can be derived from naturally occurring or synthetic materials. Naturally occurring materials currently under investigation include collagen, gelatin, fibrin, alginate, hydroxyapatite, and chitosan [16, 20-22]. Natural

polymers are biocompatible, mimic the biochemical structure of the native cellular environment, and are degradable by enzymatic or hydrolytic mechanisms [22]. Unfortunately, natural materials have many disadvantages, including relatively high antigenicity, batch to batch variation, and increased risk of transfer of infectious disease. The most widely used synthetic materials in tissue engineering applications are polymers [16, 17, 21, 22]. Synthetic polymers are desirable because they have very little variability from batch to batch, have a wide spectrum of properties, and have tunable degradation rates. These materials can also be processed into a variety of shapes, such as sponges, films, and microspheres.

Absorbable and Degradable Polymers

Absorbable polymers are those plastics that are degraded and removed from the body, while degradable polymers are remodeled and remain in the body. One of the well known, synthetic absorbable polymers used is polylactide (PL) [16]. The US Food and Drug Administration has approved PL for human use in absorbable sutures and some implantable devices. PL has various forms, including poly-L-lactide (PLL), poly-D-lactide (PDL) and poly-D,L-lactide (PDLL). PLL and PDL are semicrystalline polymers while PDLL is an amorphous polymer. All three forms degrade through hydrolysis to lactic acid, a normal metabolite that is found in the body and is excreted from the body as water and carbon dioxide. Select material properties that determine the rate of hydrolysis are outlined in Table 1.1. Sterilization method and environmental factors such as biochemical agents, pH, and temperature will all influence the rate of hydrolysis.

Polylactides can be made with a variety of properties, allowing them to be used in a large range of applications. PL can be fabricated into many forms, such as sponges [16], woven or knit meshes [16], microparticles [23], and films [24]. For PL to be successfully used as a cellular substrate for adipose tissue engineering, preadipocytes and adipocytes must be able to adhere to and proliferate and/or differentiate on the scaffold. Conejero and coworkers seeded fat-derived stem cells onto a PL scaffold and showed that the cells were able to grow and form a tissue [25]; however, PL is not an ideal scaffold to use as a cell carrier because it is hydrophobic and releases acidic byproducts as it degrades, causing the pH of the local environment to decrease. Even though cells do eventually grow on PL, surface modification of this polymer could allow the cells a more hospitable surface, leading to immediate cell growth.

Table 1.1 Select material properties determining hydrolytic degradation of absorbable polymers

Crystallinity
Hydrophobicity/ hydrophilicity
Molecular weight
Porosity
Structure

Synthetic materials alone will likely not create a proper cellular environment. Natural materials combined with synthetic materials likely provide the ideal environment for cells, i.e. an environment that is structurally sound and conducive to adhesion and proliferation. Collagen, a degradable material that is remodeled *in vivo* by collagenase, has been widely used in medical applications for many years and plays an important role in the formation of tissues. Collagen is a crosslinked protein found throughout the human

body that is biodegradable, nontoxic, and has weak antigenecity. The properties of collagen are directly affected by the density of crosslinking and the type of crosslinking agent employed [26]. Glutaraldehyde is the most commonly used crosslinking agent because it is inexpensive and provides sustained long-term durability by creating a high density of covalent crosslinks [26, 27]. Unfortunately, this chemical is thought to cause long-term cytotoxicity as well as calcification. If no crosslinking agent is used, collagen is degraded in the body too quickly to be clinically viable.

Tannic acid is a plant polyphenol that has the ability to crosslink proteins and is rumored to have anti-carcinogenic properties. Tannic acid is capable of crosslinking proteins because it contains a large number of functional groups. Specifically, hydrogen bonds form between the phenolic hydroxyl groups on the tannic acid and the carboxyl groups of the protein [28] thus binding the protein. Hydrogen bonds are lower energy bonds than covalent bonds; therefore, a tannic acid crosslinked collagen will degrade relatively fast as compared with a glutaraldehyde crosslinked collagen. Tannic acid is reported to be an anticarcinogen for certain types of cancer, including mammary cancer, and is an effective inhibitor of tumors in mice [28]. Tannic acid crosslinking allows the collagen to degrade within a reasonable time, while also potentially reducing the chances of tumors recurring.

Composite Injectable Systems

An injectable composite system is of particular interest because it is mechanically similar to soft tissue, conforms to irregular spaces, and may be implanted in a minimally invasive manner [29]. The composite system is composed of two distinct parts, a rigid absorbable scaffold for cell attachment and growth, and an absorbable gel to facilitate the scaffold delivery, as shown in Figure 1. The scaffold should have a diameter smaller than the gauge of a needle in order to allow injection. This tissue engineering strategy can be modified so scaffolds of varying properties are embedded within the same hydrogel to obtain a tunable drug delivery system and tailored absorption profile. Composite systems, by virtue of their discrete scaffold structure, allow tissue integration and vascularization within the construct as well as serial implantation, and thus may allow the reconstruction of larger volumes of tissue than the traditional continuous scaffolds which are diffusion limited [29].

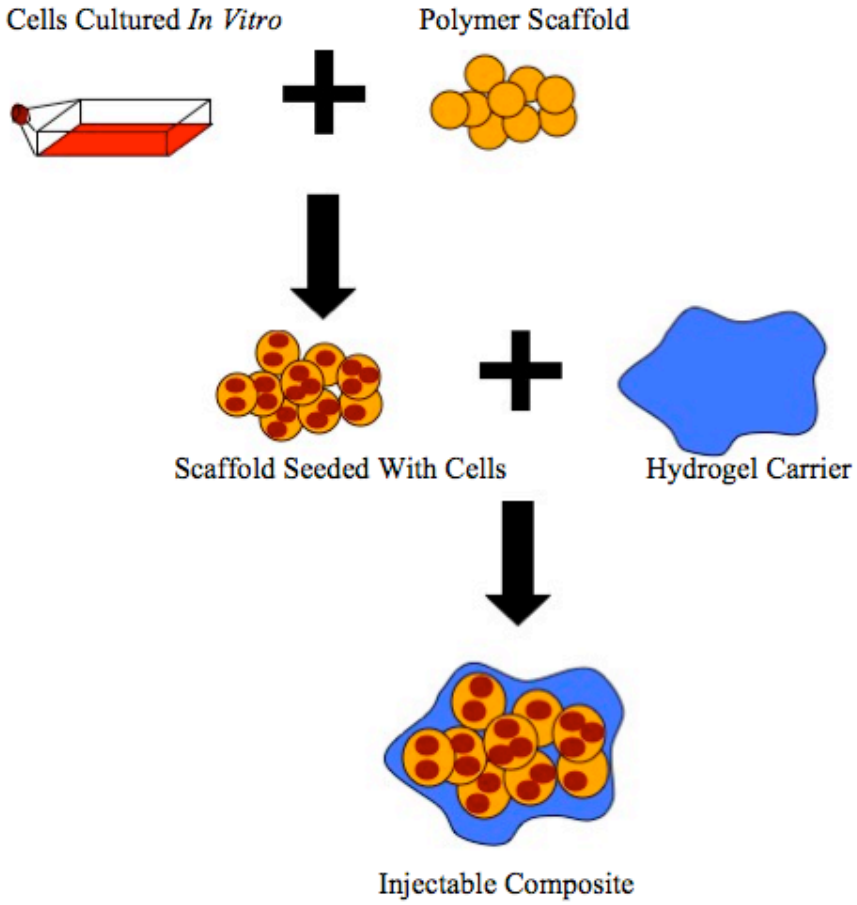

Figure 1.1 The development of injectable composite devices for breast tissue reconstruction

Maintenance of Adipose Tissue Long-Term

Collagen and PL are effective scaffolds for cell attachment and proliferation, but differentiation will be key to the long-term maintenance of soft tissue bulk. Satory and coworkers investigated the effects of conjugated linoleic acid, as a medium additive on preadipocyte proliferation and lipid filling [30]. Their results showed that certain concentrations of conjugated linoleic acid in the medium inhibited preadipocyte proliferation and increased cellular lipid content. Although there are differences between

conjugated linoleic acid and linoleic acid, there is not enough detailed research to determine the effects of each different type of linoleic acid on cellular attachment and growth. Based upon these results, this study hypothesizes that inclusion of lipid into an injectable composite system might allow preadipocytes seeded on the scaffolds to differentiate once injected into the body, while stimulating adipocytes present in the tissue to retain cellular lipid. Conjugated linoleic acid has also been shown to be anticarcinogenic in a rat mammary tumor model [31]

The long-term goal, beyond the scope of this work, is to develop an injectable biodegradable composite breast tissue reconstruction device with anti-tumor and bulking capabilities. This study focuses on designing polymer scaffolds that are viable for preadipocyte growth and differentiation. Polylactide beads were coated with collagen and linoleic acid, then seeded with preadipocytes and observed *in vitro* to assess cell attachment, growth, and differentiation patterns.

MATERIALS AND METHODS

To meet the objectives of this research, two primary studies were performed. The first study determined cell viability on collagen encapsulated polylactide beads. The second study examined cell viability and differentiation on collagen coated polylactide beads and collagen and linoleic acid coated polylactide beads. Metabolic activity, lipid and fatty acid production, cell viability, and gene expression of cells were compared between the coated polylactide beads, uncoated polylactide beads and 2-D surfaces.

Polylactide scaffolds

Solution Preparation for Emulsion-Solvent Evaporation

Polylactide (PL) pellets were obtained from DOW chemicals (DOW LLC, Minneapolis, MN). A 10% w/v solution of PL was prepared by dissolving 2 grams of PL pellets into 20 mL of dichloromethane (Mallinckrodt Inc., Hazelwood, MO) for 48 hours. A 0.3% solution of PVA was created by adding 3 grams of PVA flakes (Sigma-Aldrich, St. Louis, MO) into 1000 mL of distilled water, then stirring and heating the solution over low heat until the PVA was completely dissolved. The solution was then cooled to room temperature before use. A 2% isopropanol solution was prepared by mixing 20 mL of isopropanol (VWR, West Chester, PA) with 980 mL of distilled water.

Fabrication Equipment and Procedure

Scaffolds were prepared using an emulsion-solvent evaporation procedure. A glass tank measuring 24 cm in diameter and 28 cm in height, with a drain located in the

bottom that was covered with a brass WireMesh® screen (Paragona®, Stockholm, Sweden), was elevated on two 2" x 4" risers. Tygon R-3603 tubing (Saint-Gobain Performance Plastics, Akron, OH) was connected to both the drain at the bottom of the tank and to the drain in the chemical hood. A paddle stir rod connected to a EUROSTAR power control-visc overhead stirrer (IKA® Works, Wilmington, NC) was placed over the tank. A solution of 1000mL of 0.3% PVA and 5000mL of distilled water were mixed together in the tank to form a 0.05% v/v solution of PVA. The solution was stirred for 5 minutes at 200 rpm.

Twenty mL of 10% PL solution were then poured into a 20cc syringe (BD, Franklin Lakes, NJ) with an attached 16-gauge needle (BD). The needle was submerged in the 0.05% PVA solution near the vortex created by the stir rod, and the PL solution was injected into the PVA solution. The solution of PVA and PL was stirred for 10 minutes at 275 rpm. Once the microspheres were settled to the bottom of the tank, 2/3 of the PVA solution was drained. Two liters of 2% isopropanol solution were added to the tank, and then stirred for 5 minutes at 200 rpm to wash the microspheres. The tank was drained until approximately 1 liter remained. The microspheres and liquid were then transferred to a 1L glass Pyrex® bottle (Corning, Inc., Corning, NY) using a vacuum source connected to a 45 mm 3-Port for medium bottles (Bellco Glass, Inc., Vineland, NJ) by Tygon tubing (Saint-Gobain Performance Plastics). The liquid in the bottle with the microspheres was removed, and replaced with 200 mL of fresh 2% isopropanol solution. The bottle was then placed on an orbital shaker (IKA® Works) and shaken at 150 rpm overnight at room temperature. The microspheres were then dried on a Coors®

Bichner filter funnel (Fisher Scientific, Fair Lawn, NJ), which had a cellulose grade 1 filter paper (Whatman®, Florham Park, NJ) in place. The filter funnel was inserted into a 500 mL Kimax Erlenmeyer filter flask (Chemglass, Vineland, NJ) and connected to a compressed air system. The air was circulated over the microspheres for a few hours, until the microspheres were completely dried, as evidenced by their shiny appearance. The dry microspheres were transferred to a scintillation vial (Fisher Scientific) and stored under vacuum.

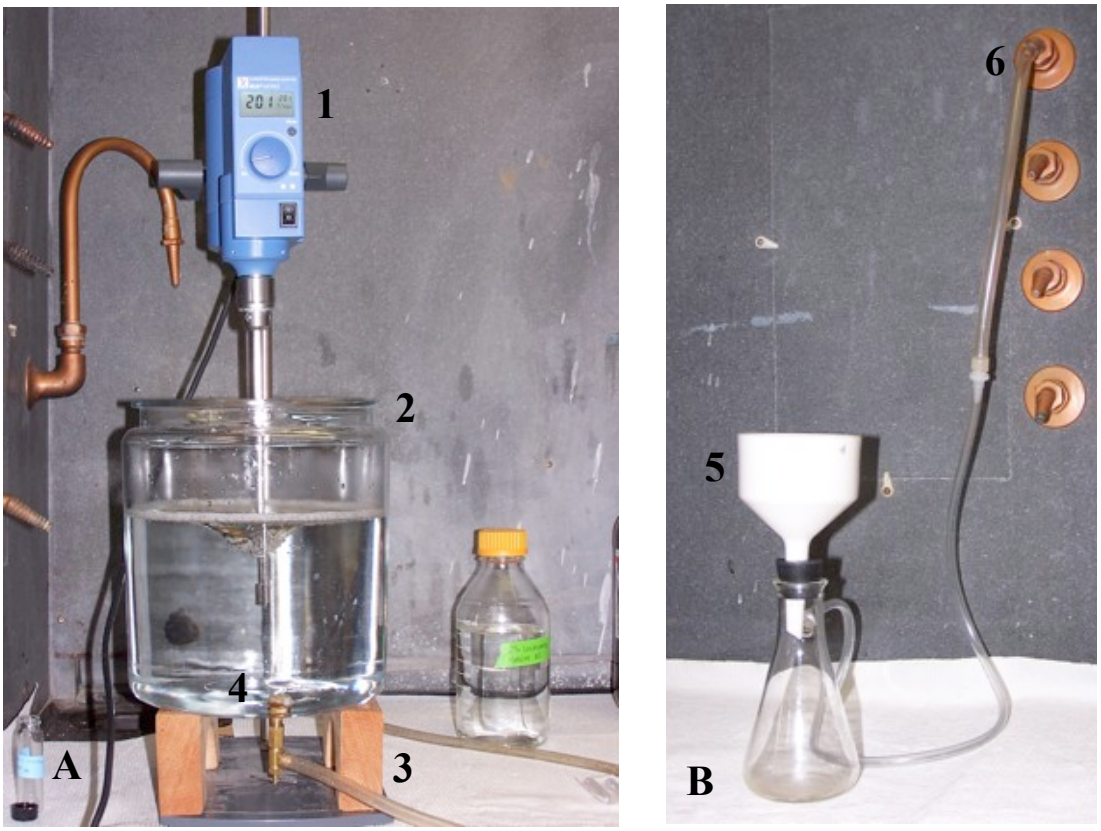

Figure 1.2 PL scaffold fabrication setup: overhead stirrer (1), glass tank (2), drainage tubing (3), drain with mesh cover (4) (A); filter setup to dry PL scaffolds: Buchner funnel (5), and compressed air (6) (B)

Polylactide Microspheres with Entrapped Collagen

Collagen (Invitrogen, Carlsbad, CA) was solubilized by adding 1.5 mL of collagen to 167 μm of 10x DPBS (Invitrogen), 225 μL fetal bovine serum (FBS) (Mediumtech, Herndon, VA), 358 μL 1 x Dulbecco's Modified Eagle's Medium (DMEM) (Invitrogen), and 20 μL 1N NaOH, creating 2.27mL of solubilized collagen. Two ratios of collagen to PL pellets were mixed, 50% collagen to 50% PL, referred to as solution A, and 75% PL to 25% collagen, referred to as solution B. For solution A, 2.27

mL of solubilized collagen was mixed with 5 mL of dichloromethane (Mallinckrodt Inc.) and 1 gram of PL pellets (Cargill DOW LLC) in a scintillation vial (Fisher Scientific) for 48 hours. For solution B, 2.27 mL of solubilized collagen was mixed with 6.75 mL of dichloromethane and 1.35 grams of PL pellets in a scintillation vial for 48 hours. PVA solution and 2% isopropanol solution were prepared as previously described. Microspheres from these solutions were created using the emulsion-solvent evaporation technique outlined previously.

Polylactide Microspheres Coated with Collagen

PL microspheres were created using the emulsion-solvent evaporation technique outlined previously. A mixture of 6 grams of hexanediamine with 100 mL of isopropanol created a 6% hexanediamine/isopropanol solution. To create a 0.1% tannic acid solution, 0.1 gram of tannic acid was added to 100 mL of distilled water and the solution was stirred and heated to a simmer. The solution was then allowed to cool to room temperature before use. A collagen/acetic acid solution was created by adding solubilized collagen to 3% acetic acid (Fisher Scientific) at a ratio of 2:1.

The microspheres were stored under vacuum for 3 Days and then added to a 6% hexanediamine/isopropanol solution and immersed into a 60°C water bath for 10 minutes. The solution was shaken continuously while in the water bath, to prevent the beads from adhering to the bottom of the flask. The microspheres were placed on a cellulose grade 1 filter paper that was placed on a Coors® Bichner filter funnel that was inserted into a 500 mL Kimax Erlenmeyer filter flask, and washed extensively with

deionized water. The microspheres were dried at room temperature under vacuum for several hours. Once dried, the microspheres were immersed in 0.1% tannic acid solution at room temperature for 3 hours, and then washed extensively with deionized water. The microspheres were then immersed into a 2:1 collagen/acetic acid solution for 24 hours at 4°C, with occasional shaking. After being washed with deionized water, the microspheres were placed under vacuum until use. These beads will be referred to as PL+C beads.

Polylactide Microspheres Coated with Collagen and Linoleic Acid

PL microspheres were created using the emulsion-solvent evaporation technique outlined previously. A mixture of 6 grams of hexanediamine and 100 mL of isopropanol created a 6% hexanediamine/isopropanol solution. To create a 0.1% tannic acid solution, 0.1 gram of tannic acid was added to 100 mL of distilled water, and the solution was stirred and heated to a simmer. The solution was then allowed to cool to room temperature before use. A collagen/acetic acid/linoleic acid solution was created by adding solubilized collagen to 3% acetic acid at a ratio of 2:1 to a volume of 3 mL, then 1 mL of linoleic acid bound to bovine serum albumin (Sigma-Aldrich) was added to the solution and stirred.

The microspheres were stored under vacuum for 3 Days and then added to a 6% hexanediamine/isopropanol solution and immersed into a 60°C water bath for 10 minutes. The solution was shaken continuously while in the water bath to prevent the beads from adhering to the bottom of the flask. The microspheres were placed on a

cellulose grade 1 filter paper that was placed on a Coors® Bichner filter funnel and inserted into a 500 mL Kimax Erlenmeyer filter flask, and washed extensively with deionized water. The microspheres were dried at room temperature under vacuum for several hours. Once dried, the microspheres were immersed in 0.1% tannic acid solution at room temperature for 3 hours, and then washed extensively with deionized water. The microspheres were then immersed into a collagen/acetic acid/linoleic acid solution for 24 hours at 4°C, with occasional shaking. After being washed with deionized water, the microspheres were placed under vacuum until use. These beads will be referred to as PL+C+L beads.

Cell Culture

Stir Flask

DMEM (Invitrogen) was supplemented with Fetal Bovine Serum (FBS), L-glutamine, fungizone, and antibiotic-antimycotic. Six Wheaton Celstir spinner double side arm flasks (Fisher) were used; three flasks for PL beads, and three flasks for PL beads with entrapped collagen. The walls of the stir flasks were coated with 0.15% agarose solution (Sigma-Aldrich) to prevent the cells from adhering to the walls of the flasks. 3T3-M mouse fibroblasts were cultured with supplemented DMEM in a Wheaton Celstir spinner double side arm flask (Fisher). To each stir flask containing 50 mL of supplemented DMEM medium, $4x10^6$ cells, and 1.75 mL of either PL beads or PL beads with entrapped collagen were added. Assays were performed at Day 7 and Day 13.

2-D Cell Culture

3T3-L1 mouse preadipocytes were cultured on 12-well polystyrene plates (Corning® Inc.) with 1.5 mL of DMEM-C (Invitrogen) in each well. Initially, $3.125x10^5$ cells were seeded in each well. The cells were cultured at 37°C and 5% CO_2, and the medium was changed every 2 Days.

3-D Cell Culture

3T3-L1 cells were cultured with DMEM-C (Invitrogen) on 12-well ultra low cluster plates. The wells were coated with 0.15% agarose solution (Sigma-Aldrich) to prevent the cells from adhering to the wells. To each of 4 wells, 100 μg of microspheres, $3.1x10^5$ cells, and 1.5mL of DMEM-C were added. The microspheres tested in this assay were the PL beads, PL+C beads, and PL+C+L beads. Assays were performed at Days 4, 10, and 18 using 4 wells per microsphere type per plate. Figure A-1 shows which wells were designated for each scaffold type and assay.

Material Analysis

Microsphere Characterization

PL microspheres with entrapped collagen were characterized using Fourier Transform Infrared Spectroscopy (FTIR), and Gomori's One Step Trichrome. Also, the microspheres were examined and measured using an inverted microscope.

Fourier Transform Infrared Spectroscopy

FTIR was performed to identify if collagen was present in the collagen encapsulated microspheres. The samples were placed onto the Thermo-Spectra-Tech Foundation Series Diamond ATR (Thermo Fisher Scientific, Inc., Waltham, MA), and compressed with the compression tower of the Diamond ATR.

FTIR spectra were collected using a Thermo-Nicolet Magna 550 FTIR spectrophotometer (Thermo Fisher Scientific, Inc., Waltham, MA) equipped with a Thermo-Spectra-Tech Foundation Series Diamond ATR (Thermo Fisher Scientific). The samples were scanned 16 times at a resolution of $4cm^{-1}$ from 4000 cm^{-1} to 525 cm^{-1} and ratioed against a background scan collected at the same parameters. The data was analyzed using OMNIC ESP version 6.1a software.

Gomori's One Step Trichrome

Gomori's One Step Trichrome was used to determine if collagen was present in the beads. The beads were placed in Bouin's fixative (Fisher) overnight. The beads were then washed with distilled water until the water ran clean then placed in Gomori's One Step Trichrome stain for 20 minutes. Then beads were transferred directly into 0.5% aqueous acetic acid for 2 minutes then differentiated in 1% aqueous acetic acid for 1 minute. The beads were rinsed in distilled water and dehydrated in 95% ethyl alcohol then absolute alcohol. The beads were examined under a steromicroscope and collagen presence showed as a green coloring on the beads, which was measured qualitatively.

PL coated scaffold properties were characterized using gel permeation chromatography, (GPC) (Waters, Milford, MA), differential scanning calorimetry (DSC) (TA Instruments, Inc., New Castle, DE), and gas chromatography (GC) (Agilent

Technologies, Foster City, CA). The samples tested included PL pellets, PL scaffolds, PL scaffolds coated with collagen, and PL scaffolds coated with collagen and lipid.

Gel Permeation Chromatography

GPC was conducted to determine the molecular weight and polydispersity of select PL scaffolds using a Waters HPLC system (Waters), consisting of a Model 610 HPLC pump, a Waters Model 486 UV/Vis detector, and a Waters Model U6K injector. The samples were dissolved in HPLC grade chloroform (Burdick and Jackson, Miskegon, MI) at a concentration of 3mg/mL of sample to chloroform.

Differential Scanning Calorimetry

The Thermal properties of the PL were determined using a DSC Thermal Analyst 2000 (TA Instruments, Inc.). The sample weight ranged from 5-10 mg and the samples were contained in aluminum pans (Perkin Elmer, Wellesley, MA). The samples were heated at a rate of 10°C/minute from 25°C to 200°C in the first cycle. The samples were then quenched using liquid nitrogen. Samples were reheated a second time to 200°C at a rate of 10°C/minute.

Gas Chromatography

GC was used to determine the amount of fatty acid present in the linoleic acid and collagen coated PL microspheres. A sample of 0.5 mg of microspheres was weighed and placed in a test tube; volumes of 300 μL of methylene chloride (Fisher Scientific) and 1 mL of 0.5 N sodium methoxide in methanol (VWR) were added to the sample. The tube was flushed with nitrogen and heated at 90°C for 10 minutes, then cooled to room temperature. One mL of 14% boron trifluoride in methanol (EMD Chemicals, San

Diego, CA) was added to the sample and heated at 90°C for 10 minutes. After the sample was cooled to room temperature, 500 μL of GC grade hexane (Fisher Scientific) and 500 μL of GC grade hexane containing the internal standard, C23:0 methyl ester (1 mg/mL) (Sigma-Aldrich) was added to the sample. Two mL of deionized water were added to the sample and the sample was vortexed for 2 minutes, then centrifuged at 1500 *x g* for 5 minutes. The upper layer of the test tube was transferred to a test tube containing a small amount of anhydrous sodium sulfate (Fisher Scientific). The liquid was transferred to a GC vial and was run in the 6850 Series II Gas Chromatograph fitted with an autosampler (Agilent Technologies). The software used to analyze the data was Chemstation (Agilent).

Cellular Characterization

Stir Flask LIVE/DEAD

A LIVE/DEAD® Viability/Cytotoxicity Kit (Invitrogen) was used to qualitatively determine the cellular viability and the cellular attachment to the different microspheres. Under sterile conditions, the LIVE/DEAD® working solution was prepared according to the manufacturer's instructions. The scaffolds were transferred to a 24-well plate (Corning® Inc.) into separate wells. Residual medium was aspirated from the scaffolds, and the scaffolds were rinsed with 1 mL sterile PBS (Sigma-Aldrich). The PBS was aspirated and 1 mL of the working solution was added to each well. The plate was incubated for 45 minutes at room temperature and protected from light. Images of the scaffolds were captured using the Axiovert 135 fluorescent inverted microscope (Zeiss,

Thornwood, NY)), the SPOT INSIGHT color digital camera (Diagnostic Instruments, Sterling Heights, MI), and Image Pro Plus 4.5 software (Medium Cybernetics, Bethesda MD). The wells were evaluated for green fluorescence, indicating viable cells, and red fluorescence, indicating non-viable cells.

Cellular Imaging

Images of the cells on polystyrene and on each of the microsphere types were captured on Day 4, Day 10, and Day 18 using the Axiovert 135, Image-Pro 4.1 software, and a SPOT INSIGHT camera.

Lactic Acid and Glucose Measurements

Lactic acid production and glucose consumption were measured before every medium change. The lactic acid and glucose present in the medium were measured using a YSI 2700 SELECT Biochemistry Analyzer (YSI Inc., Yellow Springs, OH).

LIVE/DEAD® Assay

A LIVE/DEAD® Viability/Cytotoxicity Kit (Invitrogen) was used to qualitatively determine the cellular viability and the cellular attachment to the different microspheres. Under sterile conditions, the LIVE/DEAD® working solution was prepared according to the manufacturer's instructions. The scaffolds were transferred to a new 24-well plate (Corning® Inc.) into separate wells. Residual medium was aspirated from the scaffolds, and the scaffolds were rinsed with 1 mL sterile PBS (Sigma-Aldrich). The PBS was aspirated and 1 mL of the working solution was added to each well. The plate was incubated for 45 minutes at room temperature and protected from light. Images of the scaffolds were captured using the Axiovert 135 fluorescent inverted microscope (Zeiss,

Thornwood, NY)), the SPOT INSIGHT color digital camera (Diagnostic Instruments, Sterling Heights, MI), and Image Pro Plus 4.5 software (Medium Cybernetics, Bethesda MD). The wells were evaluated for green fluorescence, indicating viable cells, and red fluorescence, indicating non-viable cells.

Triglyceride Assay

The total intracellular triglyceride concentration was determined using a differentiation assay protocol developed by Zen-Bio, Inc (Cultured Human Adipocyte Differentiation Assay Kit, Zen-Bio, Inc., Research Triangle Park, NC). The medium was aspirated from each sample; each sample was then rinsed with 1mL of sterile PBS and the liquid aspirated. The cells were frozen at -80°C for 1 hour and then thawed at 37°C for 10 minutes. The freeze-thaw cycle was repeated twice. One mL of 1% Triton X-100 (Fisher Scientific) was added to each well to lyse the cells on the scaffolds. The scaffolds were then incubated at room temperature for 30 minutes. The triton solution with cell debris was transferred to a microcentrifuge tube and centrifuged for 10 minutes at 3000 rpm. Next, 100μL of each sample was pipetted into wells of a 96-well plate in triplicate. Glycerol standards with concentrations ranging from 0 to 200μM, shown in Table 1.2, were prepared by diluting glycerol with an appropriate volume of Nanopure water, then pipetted in triplicate into the remaining 96-well plate. Subsequently, a volume of 100μL of Infinity^{TM} triglyceride reagent (ThermoElectron Corporation, Melbourne, Australia) was added to each well of the plate that contained either a standard or a lysate sample. The plate was incubated at room temperature for 15 minutes. The absorbances of the samples in the plate were read at 490 nm using a spectrophotometer (MRX Revelation

TC, Dynex Technologies, Chantilly, VA). The resulting output included absorbances with respect to concentrations of the prepared glycerol standard solutions, and resulted in the generation of a standard curve.

Table 1.2: Glycerol Standard Concentrations

Glycerol Concentration (μM)	Amount of Glycerol (μL)	Amount of Water (μL)
0	0	350
3.125	0.38	349.62
6.250	0.76	349.24
12.5	1.50	348.50
25.0	3.03	346.97
50.0	6.1	343.90
100	12.1	337.90
200	24.2	325.80

Gas Chromatography

Transmethylation of lipid extracts was performed on each of the samples to quantify the type and volume of lipid present in the cells. Each sample underwent lipid extraction before being transmethylated. For lipid extraction, the samples were moved to a glass tube. A volume of 7.5 mL of 2:1 chloroform (Fisher Scientific) to methanol (Fisher Scientific) was added, then the tube and contents were vortexed for 3 minutes. The sample was filtered through a cellulose grade 1 filter paper (Whatman®, Florham Park, NJ) into another tube containing 0.58% $NaCl_2$ (Fisher Scientific). The original tube was then rinsed with 2.5 mL of 2:1 chloroform: methanol, and filtered into the rest of the sample. The tube was then capped and vortexed for 3 minutes, then centrifuged at 1500 rpm for 5 minutes to separate the phases. The upper layer of methanol and water

was siphoned off and discarded. The lower layer was evaporated under nitrogen to dryness. Next, the sample was transmethylated into the same tube in which the sample was evaporated. To each sample, 300μL of methylene chloride (Fisher Scientific) and 1mL of 0.5 N sodium methoxide in methanol (VWR) was added. The tube was flushed with nitrogen, capped, and heated for 10 minutes at 90°C. The samples were allowed to cool to room temperature then 1mL of 14% BFl_3 in methanol (EMD, San Diego, CA) was added to each sample. The samples were heated for 10 minutes at 90°C then cooled to room temperature. A volume of 500μL of GC grade hexane (Fisher Scientific) containing the internal standard, C23:0 methyl ester (1mg/mL) (Sigma-Aldrich) and 500μL of GC grade hexane (Fisher Scientific) was added to each tube. Subsequently, 2mL of deionized water was added to each sample and the samples were vortexed for 2 minutes. The samples were centrifuged for 5 minutes at 1000 rpm. The upper fractions of the centrifuged tube contents were transferred to a disposable glass vial containing a small amount of anhydrous sodium sulfate (Fisher Scientific) and maintained for 2 minutes. The liquid was transferred to a GC vial and flushed with nitrogen then capped and then sampled in the 6850 Series II gas chromatograph fitted with an autosampler (Agilent) and analyzed using Chemstation software (Agilent).

Reverse Transcriptase Polymerase Chain Reaction

Reverse Transcriptase Polymerase Chain Reaction (RT-PCR) analysis was used to determine if selected genes expressed by preadipocytes or adipocytes were expressed by the cells in each sample. Samples of ribonucleic acid (RNA) were tested before

culturing cells and after Day 18 of cell culture on bead scaffolds. Primers for the specific genes of interest were designed for the RT-PCR reactions.

RNA Isolation

RNA was isolated from the samples to be tested. The medium was aspirated from the cellular scaffolds and 2-D surfaces, and the samples were rinsed with 1mL of sterile PBS. The RNA was isolated from the cells using the reagents and instructions from an RNeasy Mini Kit (QIAGEN, Valencia, CA). The cell membranes of the cell samples were directly lysed in the well plates by adding 600μL of Buffer RLT (QIAGEN) to each well. Cells grown on the microspheres were lysed directly on the surface of the beads. The samples were incubated for 15 minutes at room temperature in the Buffer RLT. The lysate from each sample was then pipetted onto individual QIAshredder spin columns (QIAGEN) inserted into 2mL collection tubes. The tubes were centrifuged for 2 minutes at 13,000 rpm. After centrifugation, 600μL of 70% ethanol were added to the lysate of each sample and mixed well. A volume of 700μL of the samples was pipetted into an RNeasy mini column (QIAGEN) placed into a new 2mL collection tube. The tubes were centrifuged for 15 seconds at 13,000 rpm and the flow-through was discarded. The rest of the sample solution was pipetted onto the same mini columns, and centrifugation was repeated for 15 seconds. The flow-through was discarded again and 350μL of Buffer RW1 was added to each RNeasy column, the mixtures were centrifuged for 15 seconds at 13,000 rpm, and the flow-through was discarded. A solution of 10μL of DNase I stock solution was added to 70μL of Buffer RDD and mixed gently. The entire solution of DNase I stock/Buffer RDD (80μL) was pipetted directly onto an RNeasy silica gel

membrane and incubated at room temperature for 15 minutes. Another 350μL of Buffer RW1 was added to the RNeasy mini column, the mixture was centrifuged at 13,000 rpm for 15 seconds and the flow-through was discarded. The RNeasy column was transferred to a new 2mL collection tube and 500μL of Buffer RPE (QIAGEN) was added onto the RNeasy column, then centrifuged for 15 seconds at 13,000 rpm, and the flow-through was discarded. Another 500μL of Buffer RPE was pipetted onto the RNeasy column and centrifuged for 2 minutes at 13,000 rpm. A volume of 50μL of RNase-free water was added to the RNeasy columns and the samples were centrifuged for 1 minute at 13,000 rpm. This step was repeated and the sample RNA was collected in a 1.5mL collection tube. The final volume of each RNA sample was 100μL. All samples were stored at -80°C.

Analysis of RNA Concentration and Purity

The concentration and purity of the isolated RNA samples was analyzed using the Agilent 2100 Bioanalyzer (Agilent Technologies, Inc.), 2100 Expert Software (Agilent Technologies, Inc.) RNA 6000 Nano Assay Kit (Agilent Technologies, Inc.), RNA 6000 Ladder (Ambion, Inc., Austin, TX), and RNA 6000 Nano LabChip® (Caliper Technologies Corp., Mountain View, CA). A gel-dye mix was prepared by adding 1μL of RNA 6000 Nano dye to 65μL of filtered RNA 6000 Nano gel matrix. The gel-mix was vortexed to mix thoroughly and then centrifuged for 10 minutes at 1400 rpm. After centrifugation, 9μL of the gel-dye mix was pipetted into the G well of the LapChip®. The Chip Priming Station (Agilent Technologies, Inc.) pressurized the Chip for 30 seconds according to the manufacturer's instructions. Another 9μL of the gel-dye mix

was loaded into the 2 remaining wells on the LabChip® labeled with G. The 5μL of RNA 6000 Nano Marker was added to each sample well and ladder well. An aliquot of RNA 6000 ladder was heat denatured at 70°C for 2 minutes then 1μL of the ladder was pipetted into the ladder well on the LabChip®. The RNA samples were thawed on ice and 1μL of each RNA sample were added to the samples wells for a total volume of 6μL per well. The LabChip® was vortexed for 1 minute at 2400 rpm. The chip was inserted into the Bioanalyzer (Agilent Technologies, Inc.) and analyzed using the Eukaryote Total RNA Nano program from the 2100 Expert software (Agilent Technologies) to determine the RNA concentration, RNA integrity number, and the 28s:18s ribosomal ratio. The RNA samples were returned to -80°C storage. RNA integrity number (RIN) was measured on a scale of 0 to 10, where 10 was considered high quality RNA and any sample that had an RIN below 8 was not used.

RT-PCR Primers

Four genes were selected to test on the sample RNA. Primers were designed for the following genes for use in the RT-PCR analysis: mouse growth arrest and DNA damage inducible gene 153 (GADD 153), mouse peroxisome proliferator activator receptor-gamma (PPAR-γ), mouse adipocyte-specific fatty-acid-binding protein-2 (aP-2), and mouse beta-actin (β-actin). GADD 153 was selected to identify cells still as preadipocytes. PPAR-γ was selected as a mid marker of adipocyte differentiation and aP-2 was selected to identify cells in later stages of adipocyte differentiation. β-actin was used as a housekeeping game. A previous graduate student, Nicole Cavin, designed the primers and the primer sequences for target genes are listed in Table 1.3. The designed

primer pairs for each gene were ordered (Integrated DNA Technologies (IDT), Coralville, Iowa) and the primers were received in lyophilized powder form and each primer was resuspended in a volume of RNase-free water to provide a 30μM concentration stock primer solution. The primers were stored at -20°C.

Table 1.3: Primer Sequences for Target Genes

Taget Gene	Accession Number	Sense Primer (5'-3')	Antisense Primer (3'-5')	Amplicon Size (bp)
β-actin	NM_00393	CTGACAGACTACCTCATGAAGA	AGTACTTCACACTGCAACTGTA	305
GADD 153	X67083	CACATCCCAAAGCCCTCG	CGACTCCTCCCCTGACTC	396
PPAR-γ	NM_011146	AACCTGCATCTCCACCTTATTATTCTG	CTACCGGTGGAGAAACGAGACGAGGAC	596
aP-2	K02109	ATGTGTGATGCCTTTGTGGGA	TGTTCTCAAATACTTTCCCGT	300

RT-PCR

The relative level of gene expression in the RNA samples was evaluated using a OneStep RT-PCR Kit (QIAGEN). To prepare the RT-PCR reactions, the manufacturer's instructions were followed using a Mastercycler Gradient Thermal Cycler (Eppendorf, Hamburg, Germany). The sample RNA, primers, dNTP Mix, 5x RT-PCR Buffer, RT-PCR Enzyme Mix, and RNase-free water were thawed on ice and vortexed to mix. A gene specific master mix containing 10μL of 5x buffer, 2μL of dNTP mix, 2μL of enzyme mix, and 1μL each of the forward and reverse primer specific to the selected gene was prepared for the reactions. The appropriate volume of the master mix was distributed equally among 0.2 mL PCR reaction tubes (Fisher Scientific). An amount of 20 nanograms of template RNA was used per sample reaction. The RNA samples were diluted with RNase-free water to obtain a measurable volume of RNA that could be pipetted into each reaction tube. The final volume of each reaction sample was 50μL, reached by the addition of RNase-free water to make up the difference. The thermal cycler conditions were set to include the following steps: reverse transcription of the mRNA sample, initial activation of PCR, denaturation of the DNA double strand, annealing of the primer to the DNA strands, and extension samples.

The optimal number of cycles for denaturation, annealing, and extension was determined for each primer pair. The PCR reactions were prepared as described above. The template RNA was diluted with RNase-free water to obtain a measurable volume of RNA. No template control (NTC) samples without the template RNA were also

prepared. For the NTC samples, the total volume of 50μL was achieved by the addition of more RNase-free water.

The optimal annealing temperature for each of the primer pairs was also determined, and PCR reactions were prepared as described above. The template RNA was diluted 1:10 with RNase-free water to obtain a volume of at least 1 μL. Minus-RT control samples were prepared without the RT-PCR Enzyme Mix, and the volume was compensated with additional RNase-free water. The annealing temperature in the thermal cycler program was set at 48°C with a gradient of 5°C, in order to encompass the different annealing temperatures, for which each of the primers was evaluated.

Table 1.4 Annealing Temperatures and Cycle Numbers

RT-PCR Step	Targeted Genes	Time (Minutes)	Temperature (°C)	Number of Cycles
Annealing	B-actin	1	52.5	35
	GADD 153	1	55.3	35
	aP-2	1	53.5	35

Gel Electrophoresis

The RT-PCR reactions in the thermal cycler produced cDNA strands of each sample that were evaluated using gel electrophoresis to assess the expressed gene products. The following methods for gel electrophoresis were used to evaluate the products of the primer optimization samples as well as the RT-PCR products of the cell sample reactions. A 1X Tris Acetate EDTA (TAE) buffer was prepared by adding 900 mL of distilled water to 100 mL of UltraPure^{TM} 10X TAE Buffer (Invitrogen). A 2%

agarose gel was prepared by dissolving 2g of agarose (Invitrogen) in 100mL of 1X Tris Acetate EDTA (TAE) buffer. The agarose was heated for 2 minutes to completely dissolve the powder. Ethidium bromide (Invitrogen), at a concentration of 0.5μg/mL, was added to the agarose to stain the gel. The agarose was poured and allowed to solidify for 1 hour, creating gels with 20 wells (Horizontal Electrophoresis Systems, Fisher). The electrophoresis tray was filled with 1X TAE until the gel was completely covered. A 6X solution of bromophenol blue loading dye was prepared by adding 0.025g of Bromophenol Blue (BioRad Laboratories, Hercules, CA) to 10mL distilled water, and 3mL of glycerol (Fisher Scientific). The loading dye was added to each DNA sample to achieve a final concentration of 1X. A volume of 12μL of each sample was loaded into an individual lane of the agarose gel. A 100 base pair DNA ladder (Promega, Madison, WI) was loaded into the first lane of the gel. Electrophoresis was conducted for 2 hours at 5 kVolts per centimeter (Model FB300, Fisher Scientific). The gel was then viewed using a UV-Spectroline® BI-O-Vision™ UV/White Light Transilluminator (Spectronics Corporation, Westbury, New York) and a GEL LOGIC 100 Imaging System (Kodak, Rochester, NY). A software package, 1D Image Analysis Software (Kodak) was used to analyze the gels qualitatively and to measure the relative levels of gene expression based on the intensity of the resulting bands at the expected amplicon size.

RESULTS

Material Characterization

Stereomicroscopy

The collagen entrapped beads had an average diameter of 83μm ± 16.7μm. The beads were shiny and appeared to have bubbles beneath the surface of the beads. Most of the beads were spherical but some were oblong. Beads fixed with gomori's were examined using a stereoscope. Most of the beads had a yellow tint because of Bouin's fixative; a few beads looked green.

Polylactide beads had an average diameter of 1.02mm ± 0.21mm. They were shiny with a smooth white surface. Most of the beads were spherical but some were oblong. The collagen coated polylactide beads had an average diameter of 1.10mm ± 0.35mm. They appeared white and opaque and were spherical in shape. The collagen and linoleic acid coated polylactide beads had an average diameter of 1.11mm ± 0.27mm. The beads appeared white and opaque and were spherical in shape.

Fourier Transform Infrared Spectroscopy (FTIR)

The presence of collagen may be determined by FTIR analysis, where one would expect peaks at three amide bonding wavenumbers, 1647, 1547, and 1240. The graph shows a subtraction of the results from the PL beads from those of the PL beads with entrapped collagen. Some small peaks appear at the bonding regions for collagen, but the amplitude is not large enough to conclusively determine that collagen is present in the beads.

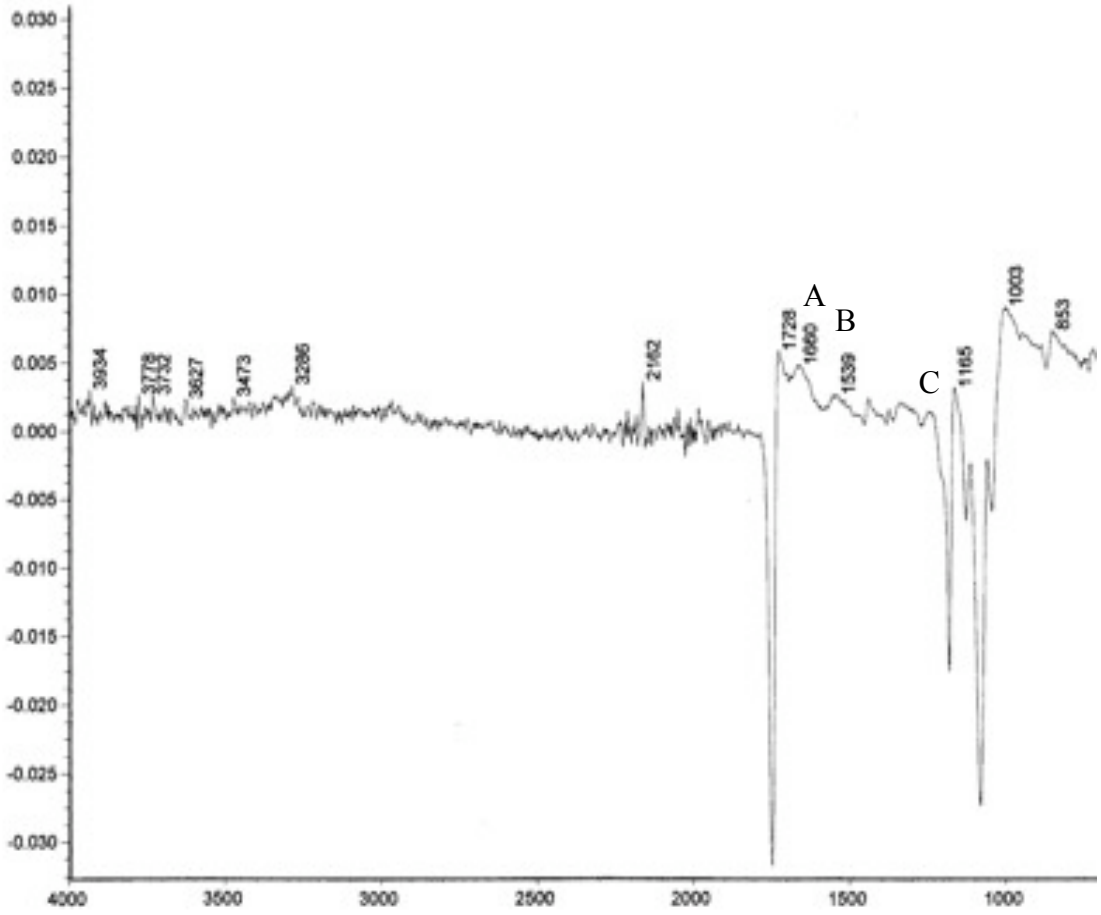

Figure 1.3 FTIR graph. Wavenumber 1647 (A), 1547 (B), and 1240 (C)

Gel Permeation Chromatography (GPC)

The weight average molecular weight (Mw) and the polydispersity of the original PL pellet and PL scaffolds were determined using GPC. The as received PL had a Mw of 193 kDaltons and a polydispersity index of 2.98 whereas the PL beads had a Mw of 205 kDaltons with a polydispersity index of 1.86. In the graphs, the first large peak is the molecular weight of the polymer. The following large peaks are solvent peaks. The as

received PL had a significantly higher ($p<0.05$) Mw than the Mw of the PL scaffold (Figure 1.4 A and B). The polydispersity of as received PL and PL scaffolds were not different ($p<0.05$).

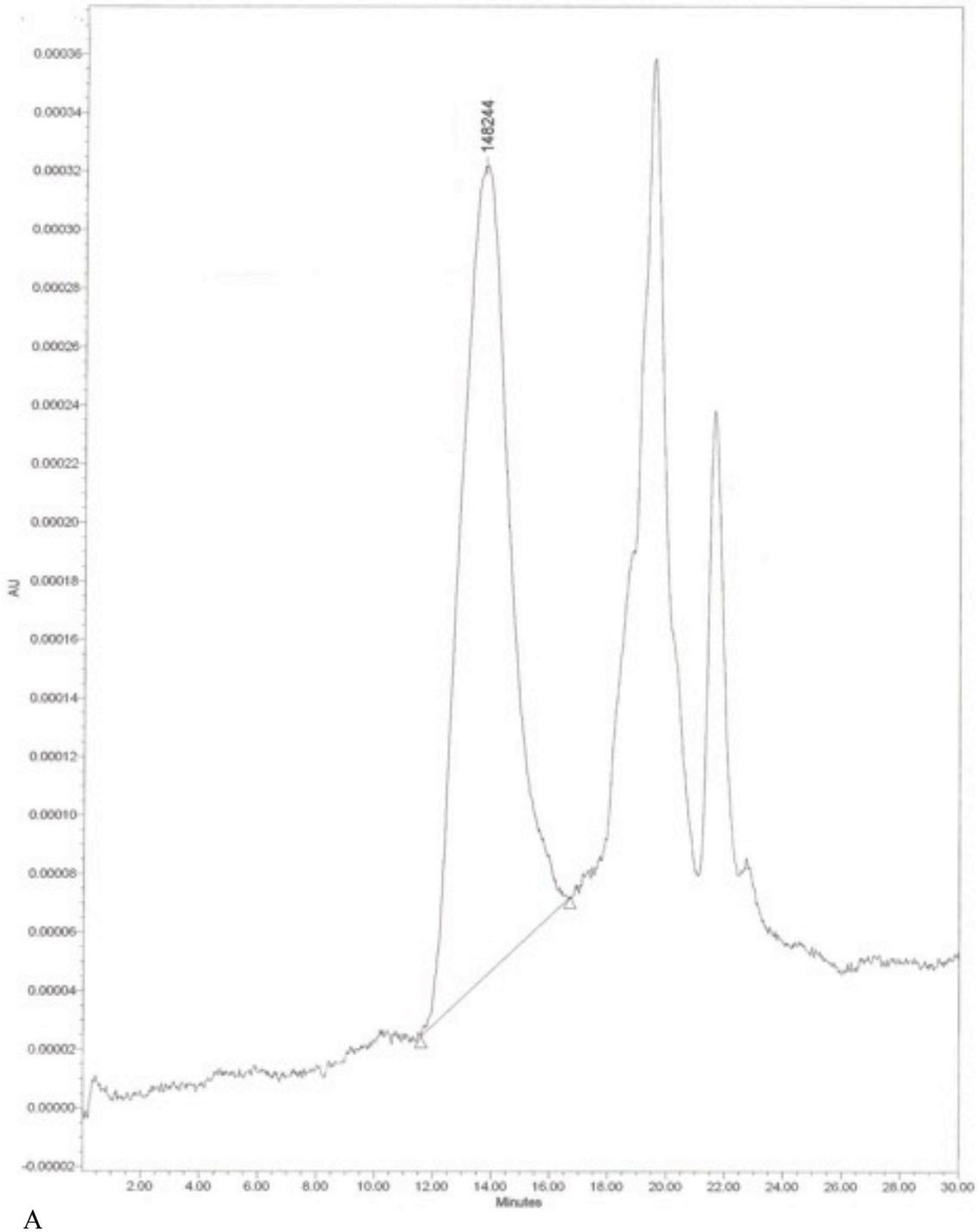

A

Figure 1.4 Sample GPC plots (A) as received PL pellet, (B) PL scaffold

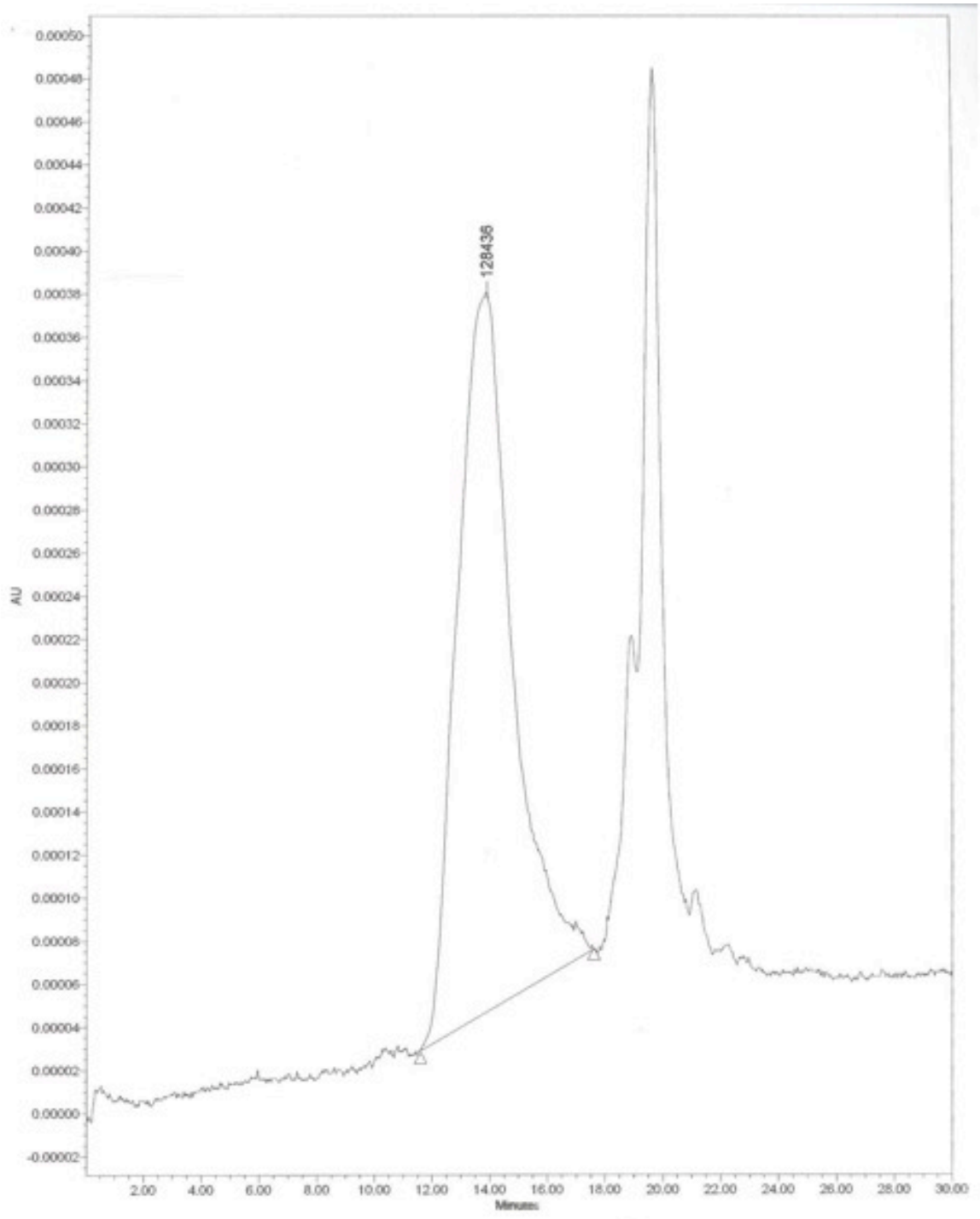

B

Figure 1.4 Sample GPC plots (A) as received PL pellet, (B) PL scaffold

Differential Scanning Calorimetry

Analysis of the as received PL pellet showed no glass transition temperature, or crystallization peak during the first or second heat but a small peak for melting temperature was present on the first heat. Analysis of the PL fabricated bead also showed no glass transition temperature, or crystallization peak during the first or second heat but a small peak for melting temperature was present on the first peak. The melting peaks for both samples were present at approximately 150°C.

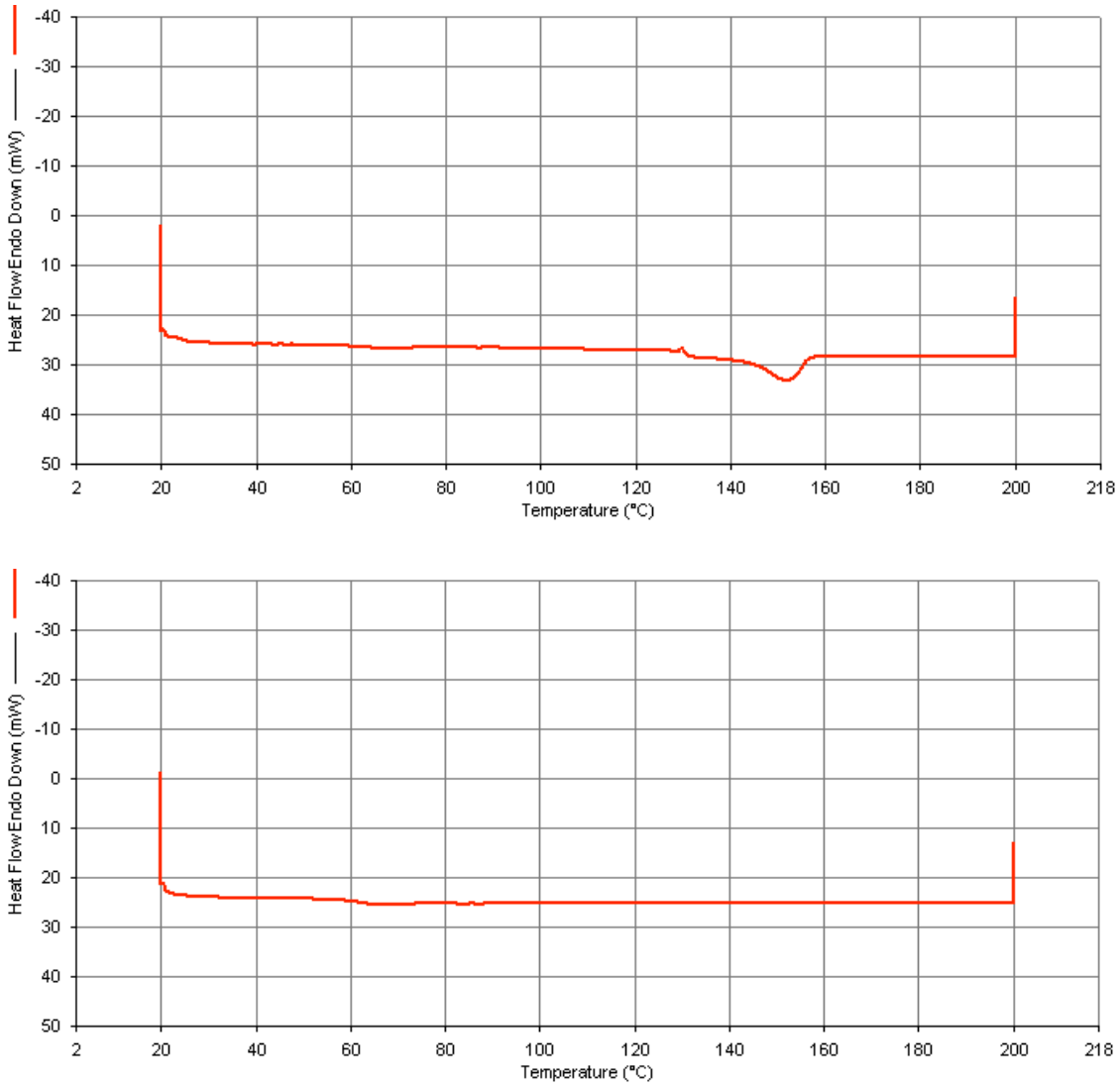

Figure 1.5 Sample DSC plots. (A) PL original pellet initial heating cycle, (B) PL scaffold first heat

Gas Chromatography

An average profile of the amount and type of fatty acid present in the beads was obtained. An internal standard was added to every sample; the corresponding peak appeared around 47 minutes. The calculations that were performed to determine the amount of total fatty acid present without the internal standard is shown below.

$\frac{Total - ISTD}{ISTD}$=Total fatty acid present

Total= total amount of fatty acid in entire sample

ISTD= internal standard added

Analysis of the PL beads revealed two fatty acids that were present in large amounts, capric acid and palmitic acid. Analysis of the PL+C beads also revealed large amounts of capric and palmitic acid. Analysis of the PL+C+L beads did not reveal a discernible peak for capric acid, but did reveal a peak for palmitic acid. The latter analysis revealed a peak for linoleic acid, as well as many more peaks than those found on analysis of the other two bead systems. The linoleic acid was also tested to determine its purity. It consisted of 90% linoleic acid and 10% other types of fatty acids.

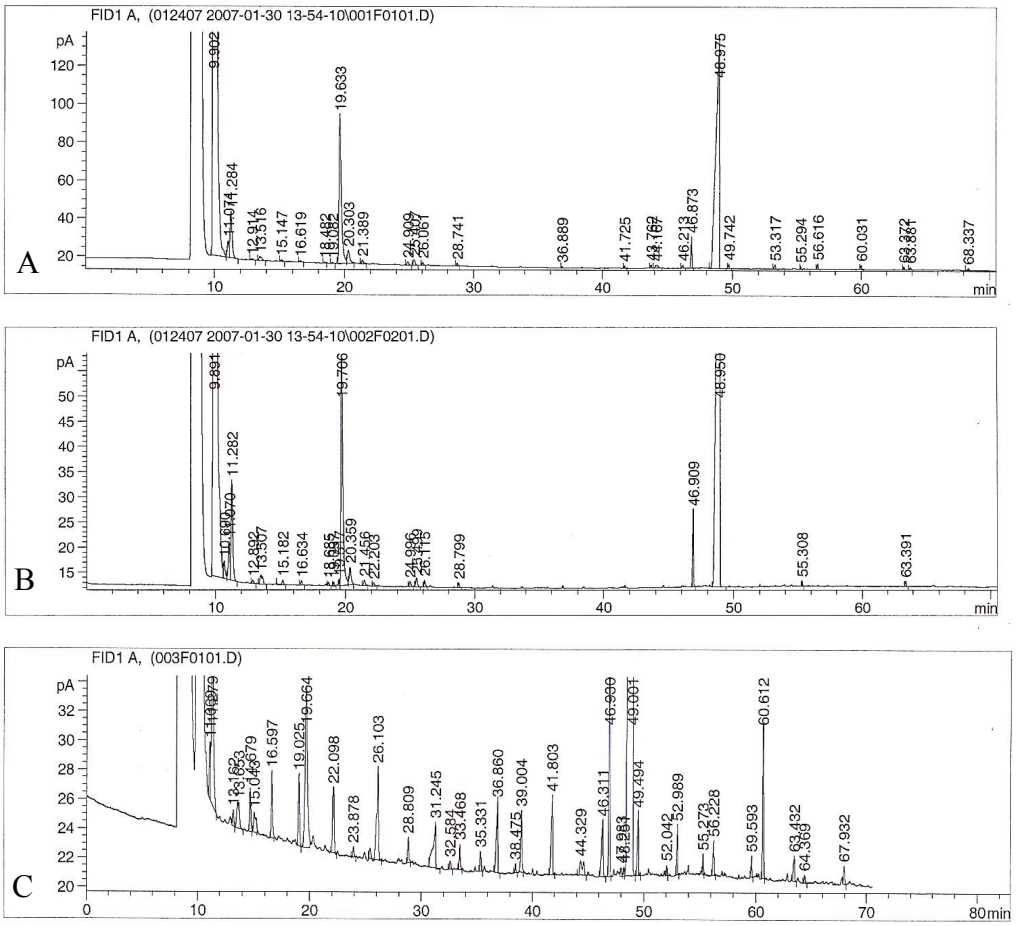

Figure 1.6 Graphs of GC results. (A) PL beads, (B) PL+C beads and (C) PL+C+L beads

Cellular Characterization

Stir Flask LIVE/DEAD

No cells attached to the PL beads by Day 7; rather the cells aggregated and floated in the medium. Cells aggregated on the some of the collagen enhanced beads, causing select beads to aggregate; however, not all of the beads supported cell attachment. By Day 13, some cells had attached to a few PL beads, mainly on the

smaller beads. Most of the PL beads with entrapped collagen were covered with cells and aggregated in large numbers.

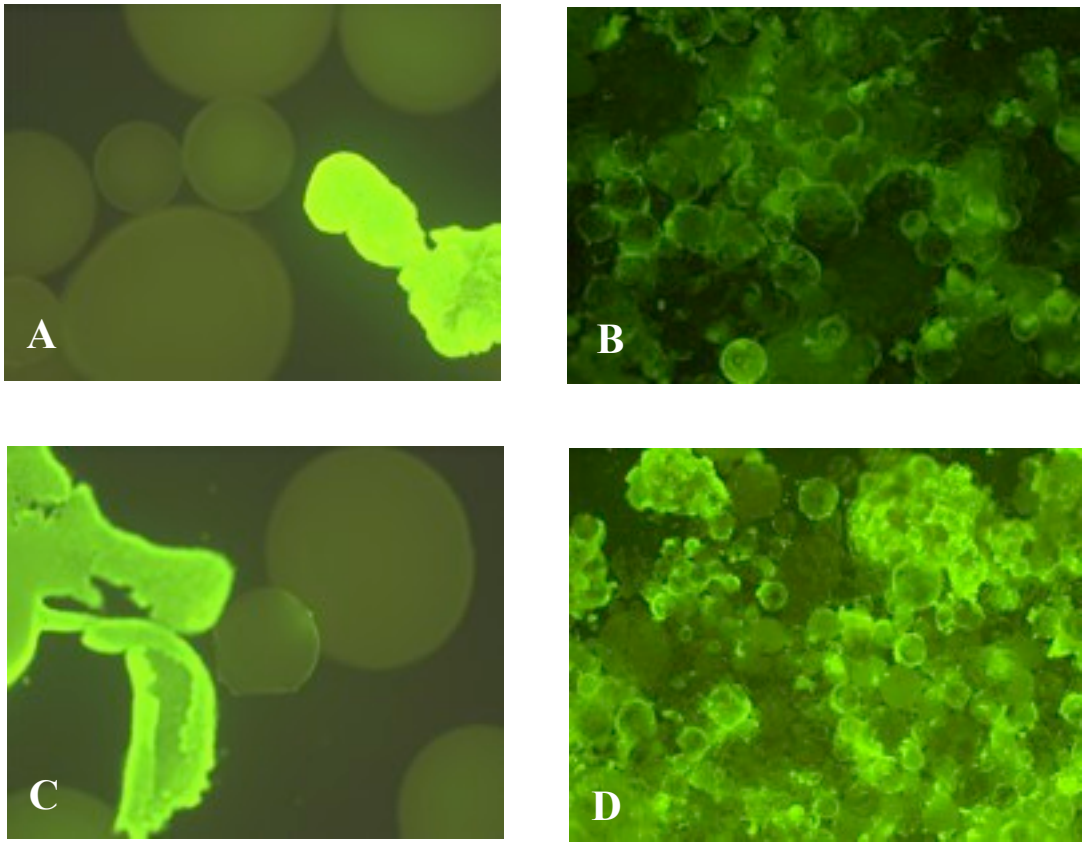

Figure 1.7 Live/Dead photographs of cells seeded on PL beads (A), PL beads with entrapped collagen (B) at Day 7, and PL beads (C) and PL beads with entrapped collagen at Day 14. All images were taken at a 50X total magnification

Cellular Imaging

Figure 3 shows the cells seeded on tissue culture treated polystyrene well plates in DMEM, i.e., the "negative controls", and shows cells seeded on tissue culture treated polystyrene well plates in DMEM supplemented with 20 μL linoleic acid, i.e., the "positive" controls. At Day 4, both cell populations were visually similar to

preadipocytes. By Day 18, cells in the negative control group appeared to produce small lipid droplets, but retained their fibroblast-like appearance. Cells cultured with 20 μL linoleic acid appeared to produce many lipid droplets, some of which coalesced into a single large lipid droplet in the cell. Many more cells in the positive control culture produced lipid by Day 18 than cells in the control culture.

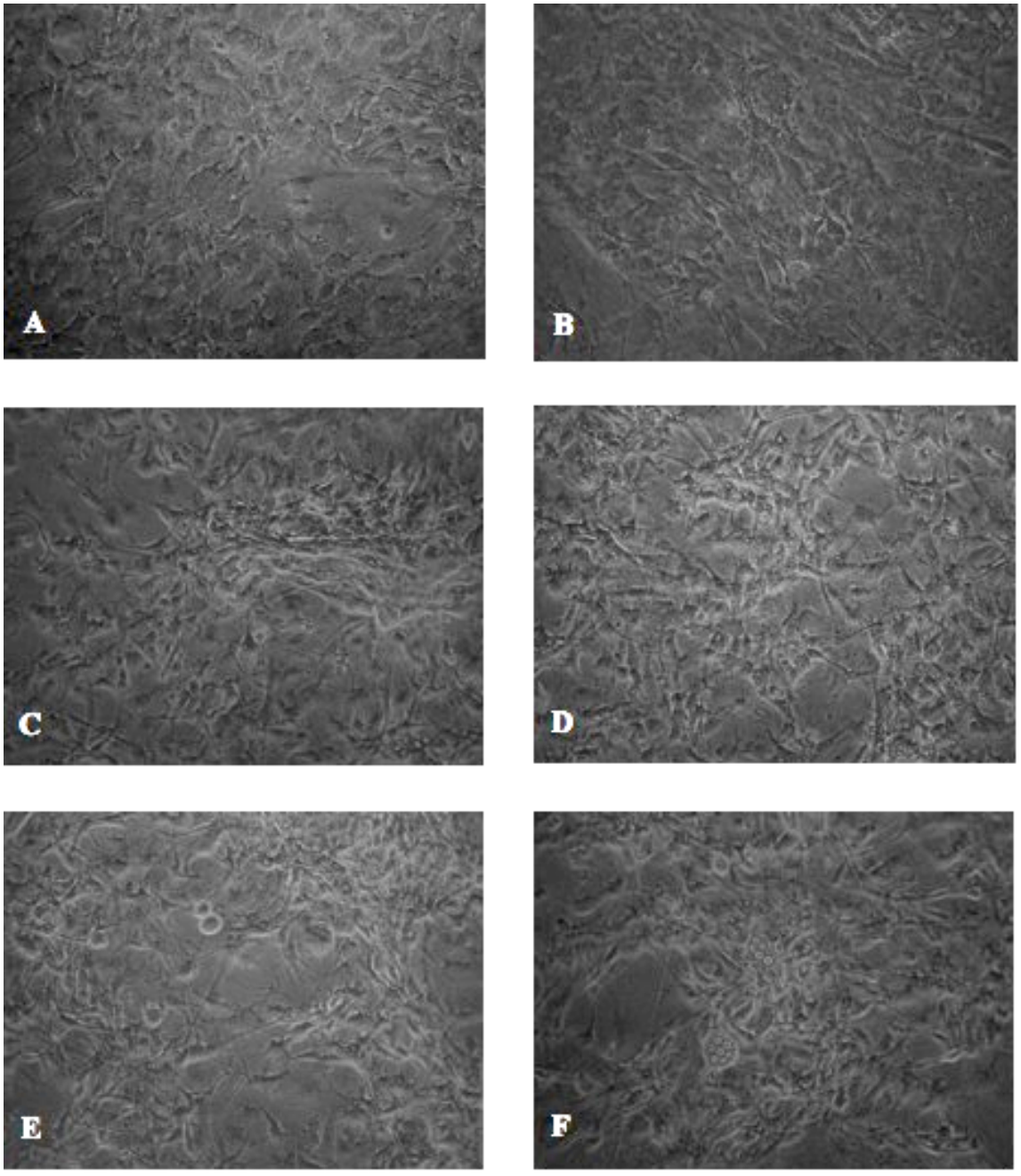

Figure 1.8 Cells seeded on polystyrene. Negative control Day 4 (A) Positive control Day 4 (B), Negative control Day 10 (C), Positive Control Day 10 (D), Negative control Day 18 (E), Positive control Day 18 (F)

Lactic Acid/ Glucose Measurements

The anaerobic metabolic activity of the cells was analyzed by testing the amount of lactic acid produced and glucose consumed by the cells at every medium change. Increases in lactic acid production indicate the cells are metabolically active. All of the samples except for PL and PL+C+L had significantly increased ($p<0.05$) the amount of lactic acid on Day 18 compared to Day 4. Between Day 10 and Day 18, all groups showed a significant increase ($p<0.05$) in the amount of lactic acid produced. The negative and positive control groups produced significantly higher ($p<0.05$) amounts of lactic acid by Day 18 than the other (experimental) samples.

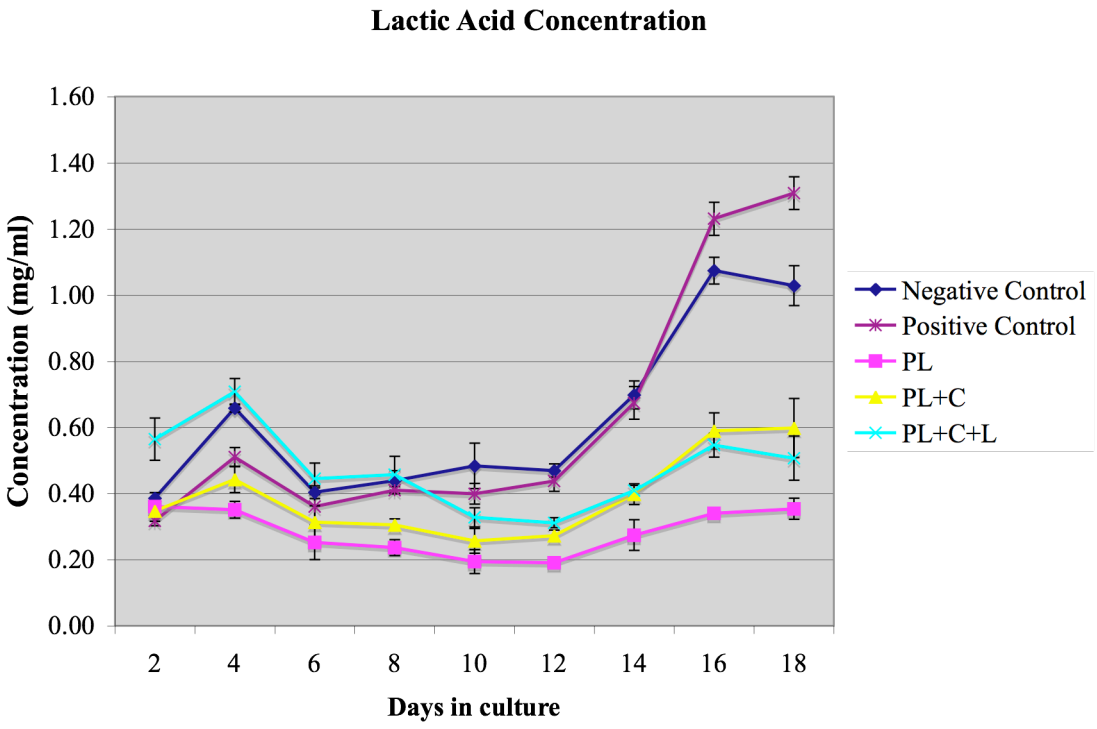

Figure 1.9 Lactic acid concentrations for the different scaffolds over 18 Days in culture. Standard deviation of 4 samples

The PL+C+L cellular group was the only group that did not have a significant decrease ($p<0.05$) in the amount of glucose between Day 4 and Day 18, although differences existed for this group between Day 2 and 18. Between Day 10 and Day 18, all groups significantly decreased ($p<0.05$) in glucose concentration. On Day 18, the negative control group and the positive control group had significantly lower ($p<0.05$) glucose concentrations than any of the other groups.

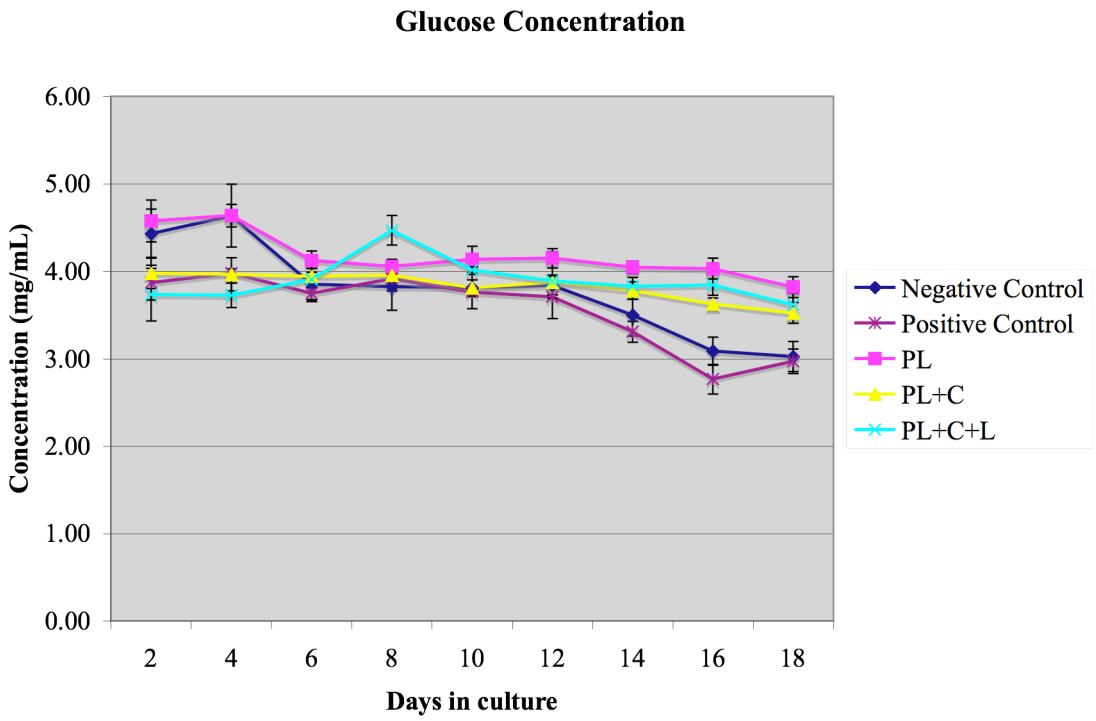

Figure 1.10 Glucose consumption for different scaffolds during 18 Days in culture. Standard Deviation of 4 samples

LIVE/DEAD Assay

Live/dead pictures were taken at Days 4, 10, and 18 for each of the 3-D scaffolds. Pictures of cell growth on Day 4 are shown in Figure 1.6. No cells visibly grew on the PL beads by Day 4, but cells grew in clusters in the medium. There were no dead beads present. Cells began attaching to the PL+C beads by this time point, and some beads were almost completely covered by live cells. Dead cells were co-localized with live cells on some beads, while others were completely acellular. The cells began to grow on the PL+C+L, almost completely covering the beads.

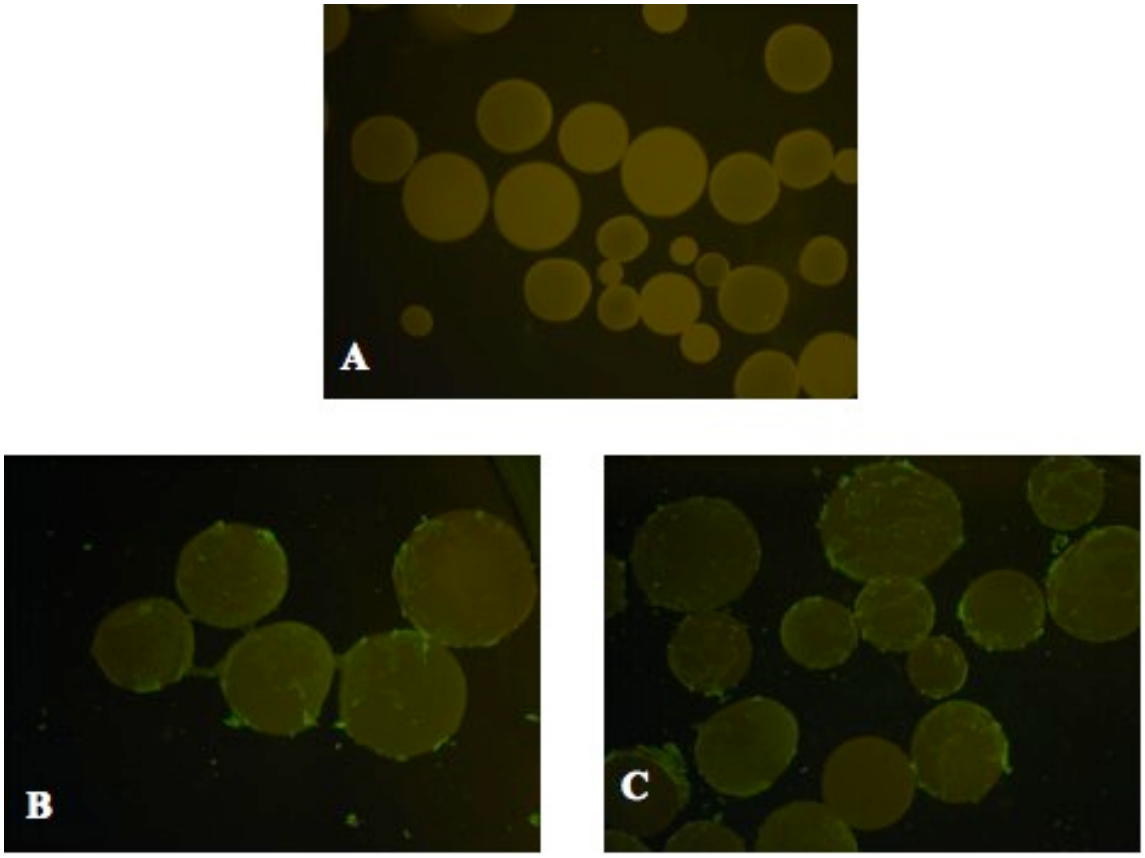

Figure 1.11 Live/Dead results showing cells seeded on PL beads (A), PL+C beads (B), and PL+C+L beads (C). All images were taken on Day 4 at 25X total magnification

Cells began growing on some of the PL beads (Figure 1.7) by Day 10. Many of the PL scaffolds did not support cell attachment. The beads that did support cell attachment also had attached dead cells. Some PL+C beads were completely covered by live cells, and almost all of the beads had some live cell attachment. A small number of dead cells were visible on the beads. Some PL+C+L beads were completely covered by live cells, and most of these beads had live cells attached. A small numbers of dead cells were visible on the PL+C+L beads.

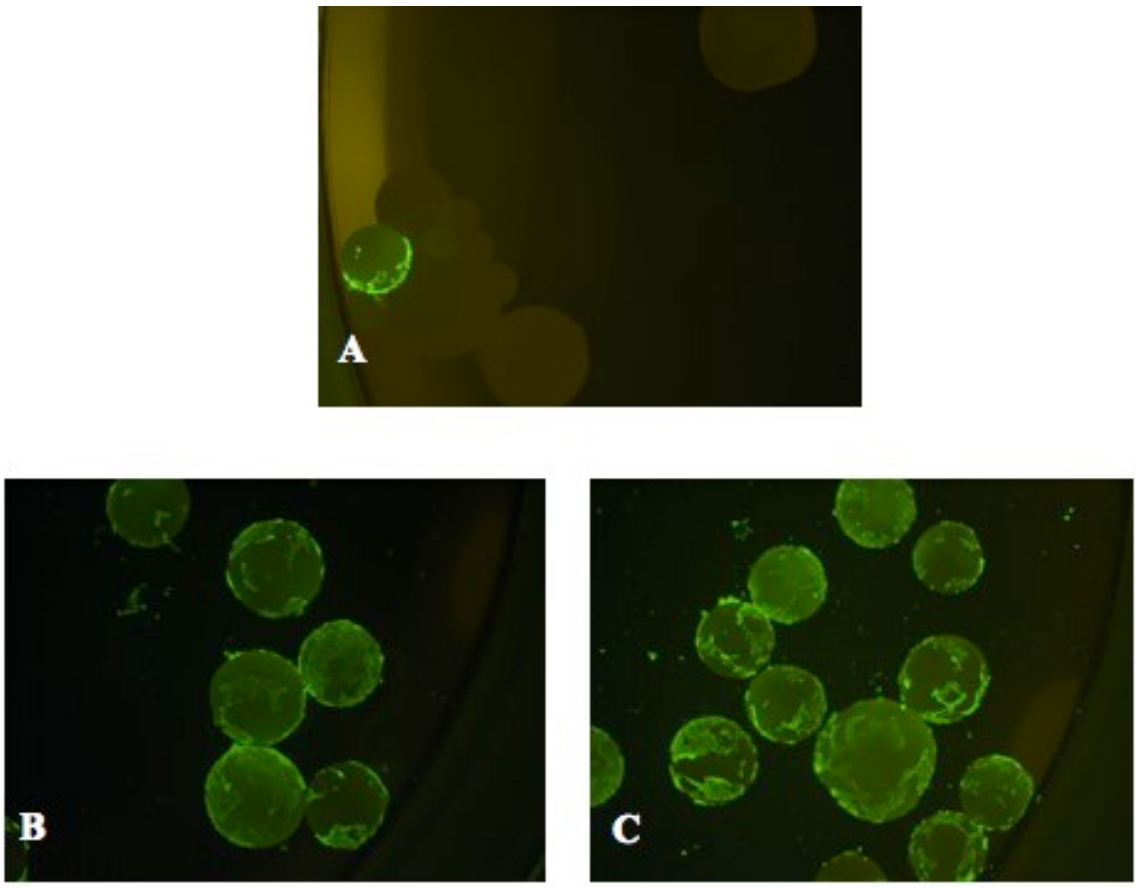

Figure 1.12 Live/Dead pictures of cells seeded on PL beads (A), PL+C beads (B), and PL+C+L beads (C). All images were taken on Day 10 at 25X total magnification

The PL scaffolds had a minimal number of beads covered with cells at Day 18 (Figure 1.8). Some of beads that had attached cells appeared to be almost completely covered with cells. Some of the attached cells bridged two or more beads. Cells were present on the PL+C beads and most of the beads appeared to be completely covered by the cells. There were more cells present on the beads than on Day 10. A minimal number of dead cells were visible on all of the beads. The PL+C+L beads also had cells present on most of the beads, where most beads appeared to be completely covered by cells. A minimal number of dead cells were visible on all of the beads.

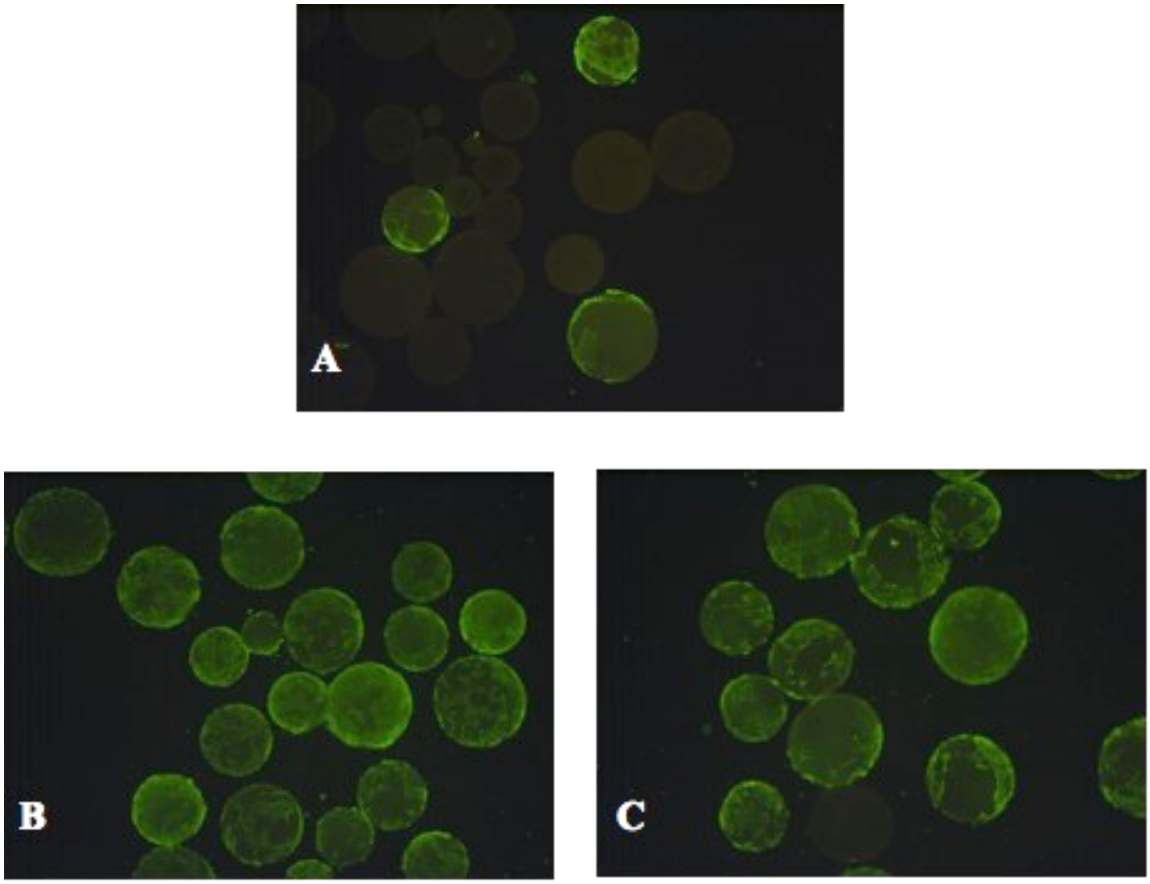

Figure 1.13 Live/Dead photographs of cells seeded on PL beads (A), PL+C beads (B), and PL+C+L beads (C). All images taken on Day 18 at 25X total magnification

Triglyceride Determination Assay

The total amount of triglyceride produced by the cells per scaffold type was determined at each time point. The triglyceride concentrations measured for each type of sample at each time point are summarized in Table 1.5. The triglyceride content for the cells seeded on the negative control, positive control, and the PL beads did not significantly increase ($p<0.05$) over the course of 18 Days. Cells seeded onto PL+C beads and PL+C+L beads, had a significant increase ($p<0.05$) in triglyceride from Day 4 to Day 18.

Table 1.5: Triglyceride Measured in Cell Samples

Day	Scaffold	Average Triglyceride Conc. (μM)
4	Negative Control	42.3 ± 5.56
4	Positive Control	41.8 ± 14.69
4	PL	48.63 ± 6.88
4	PL+C	30.4 ± 5.26
4	PL+C+L	33.63 ± 4.36
10	Negative Control	46.8 ± 3.53
10	Positive Control	42.2 ± 3.21
10	PL	53.48 ± 5.15
10	PL+C	52.04 ± 3.00
10	PL+C+L	51.7 ± 6.54
18	Negative Control	49.7 ± 4.96
18	Positive Control	51.09 ± 2.54
18	PL	39.66 ± 12.92
18	PL+C	61.29 ± 1.47
18	PL+C+L	49.4 ± 10.14

As shown in the graph, cells grown on PL beads had a significantly higher ($p<0.05$) concentration of triglyceride than cells grown on PL+C beads and PL+C+L beads by Day 4. Cells cultured with 20 μL linoleic acid (positive controls) had a significantly lower ($p<0.05$) concentration of triglyceride than the cells grown on each of the bead scaffolds by Day 10. At Day 18, cells grown on PL+C beads had a significantly higher ($p<0.05$) concentration than cells grown on PL beads and cells grown on PL+C+L beads, but had a non-significantly different concentration than the cells in the two 2-D control groups.

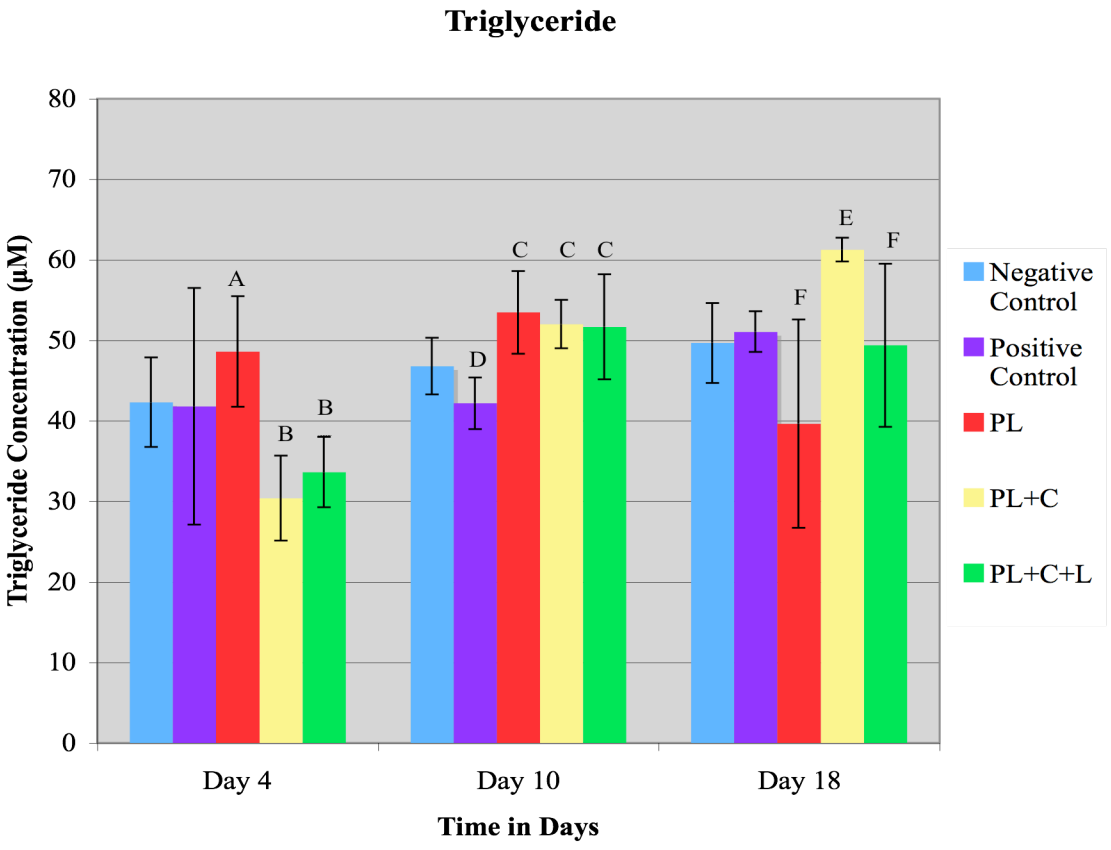

Figure 1.14 Concentrations of triglyceride produced by cells at each time point for each scaffold

Total Fatty Acid Content

The amount and type of fatty acid produced by the cells on each substrate was determined for each time point and shown in Figure 1.15. The positive control had the largest amount of fatty acid on Day 18 than any other group. These cells also had a significant increase ($p<0.05$) in the total amount of fatty acid between Day 10 and Day 18. Cells grown on PL beads had significantly decreased ($p<0.05$) in the total amount of fatty acid produced from Day 10 to Day 18. Cells grown on PL+C and PL+C+L scaffolds did not significantly ($p<0.05$) increase or decrease in the total amount fatty acid from Day 4 to Day 18. On Day 4, there were no significant differences between any of the groups. On Day 10, cells grown on the negative control scaffold had a significantly lower ($p<0.05$) amount of fatty acid than cells grown on PL beads and on PL+C beads. Also, the cells grown with 20 μL linoleic acid had a significantly lower ($p<0.05$) amount of total fatty acid than cells grown on PL+C beads. On Day 18, fatty acid content of cells grown on PL+C beads and PL+C+L beads were not significantly different ($p<0.05$) from each other, but both were significantly different ($p<0.05$) from total content of each of the other groups.

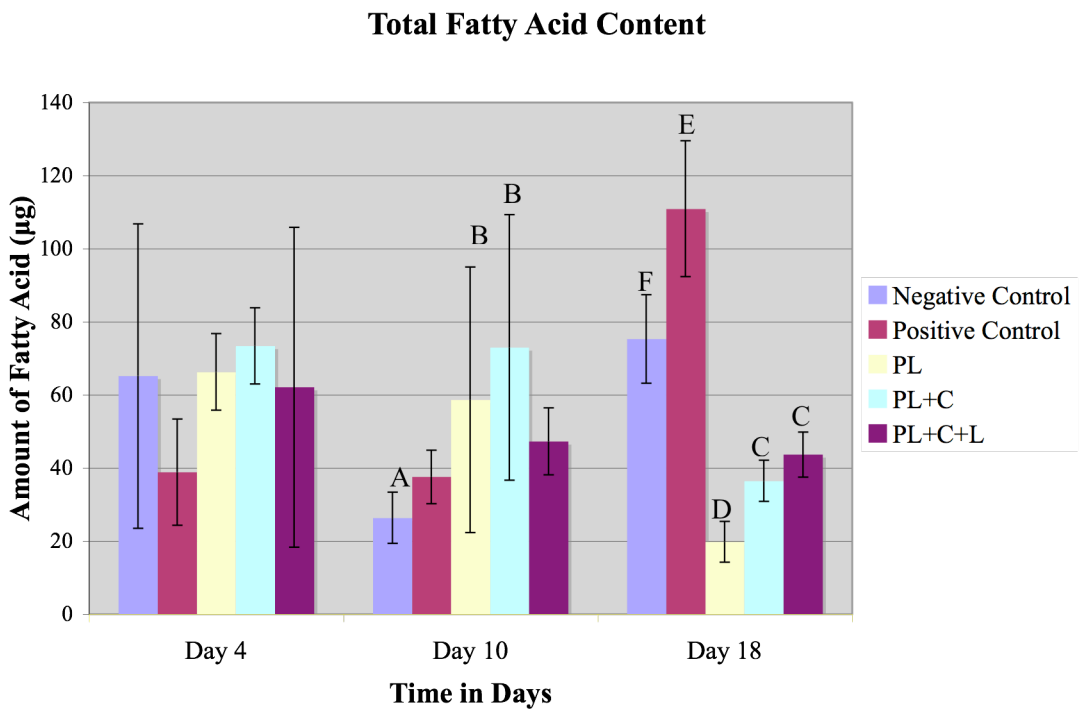

Figure 1.15 Total amount of fatty acid content in every sample at each time point

The fraction of linoleic acid that contributes to the total fatty acid content is displayed in Figure 1.16. The calculations to determine the percentage of linoleic acid in each sample are shown below.

$$\frac{(Area/ISTD)}{(Total - ISTD)/ISTD} * 100 = \text{Percentage of linoleic acid present}$$

Area= area of peak measured

ISTD= internal standard

Total= total amount of fatty acid in entire sample

No measurable amounts of linoleic acid were detected in the cells grown on the PL+C+L scaffold at any time point. One sample, with cells grown on PL scaffolds, and one sample, with cell population grown on PL+C scaffolds, had linoleic acid present on Day 10, but no other cell populations grown on these two scaffolds had linoleic acid present at any time point. Cells grown on the negative control scaffold had incorporated levels of linoleic acid on Days 4 and Day 18. There was a significant increase ($p<0.05$) in the amount of linoleic acid in the cell population grown on the control scaffold between Day 4 and Day 18. Cells cultured with 20 μL of linoleic acid (positive control) had a significantly larger ($p<0.05$) amount of intracellular linoleic acid than any other group at any time point. The amount also significantly increased ($p<0.05$) between Day 4 and Day 10.

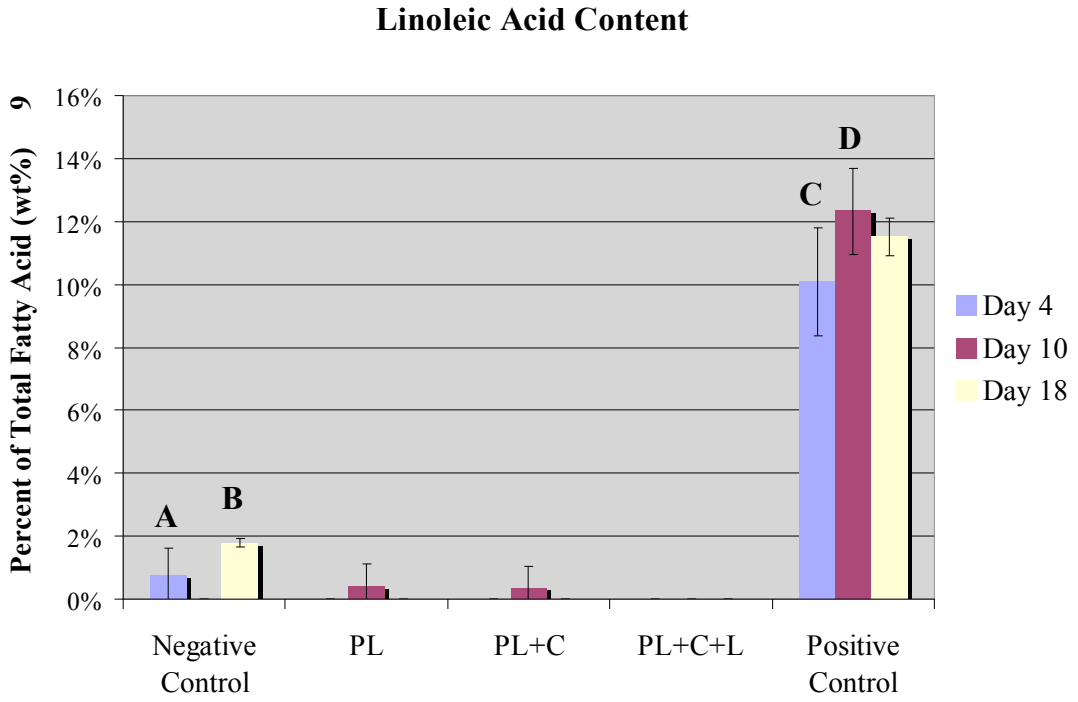

Figure 1.16 Percentage of linoleic acid in every sample at each time point

RT-PCR

RNA Purity and Concentration

The samples from the 2-D scaffolds, and from the PL+C+L scaffolds had RINs of 8 or better, but the samples from the PL and PL+C scaffolds did not have high enough RINs and were not included in further analysis. The concentration of RNA, the rRNA ratio, and the RIN for each sample for Day 18 can be found in Table 1.6. There is no evidence of DNA contamination.

Table 1.6 Bioanalyzer Results for Day 18

Scaffold	Concentration (ng/uL)	Ratio 18s:21s	RNA Integrity Number
Day 0	3	0	N/A
Control	113	2.4	10
Control	102	2.7	N/A
Control	79	23.5	10
Control	100	2.9	N/A
20uL	72	2.6	10
20uL	30	2.6	10
20uL	110	2.5	10
20uL	73	2.5	10
PL+C+L	13	3.1	9.9
PL+C+L	12	2.8	9.3
PL+C+L	10	3.0	9.5
PL+C+L	6	0	N/A

Gel Electrophoresis

All of the cell populations from the negative control, the positive control, and from the PL+C+L scaffolds expressed β-actin. The samples that did not have an RIN number also expressed β-actin. Three cell populations seeded on the negative control expressed GADD 153, while only one cell population expressed aP-2. One cell population seeded on the PL+C+L beads expressed GADD 153 while two cell populations expressed aP-2; the groups expressing aP-2 were mutually exclusive from the groups that expressed GADD 153. The cell population that expressed GADD 153 was also the same group that did not have an RIN and had a ratio of 18s:21s of zero. All four cell populations cultured in 20 μL expressed GADD 153, while only two populations expressed aP-2. PPAR-γ was not detected in any samples. Also, Day 0 samples (before seeding the cells onto scaffolds) were tested and the resulting gel showed a weak band for

β-actin, with no expression of GADD 153 or aP-2. The latter cannot be trusted because of the 0 ratio of 18s:21s and the lack of an RIN.

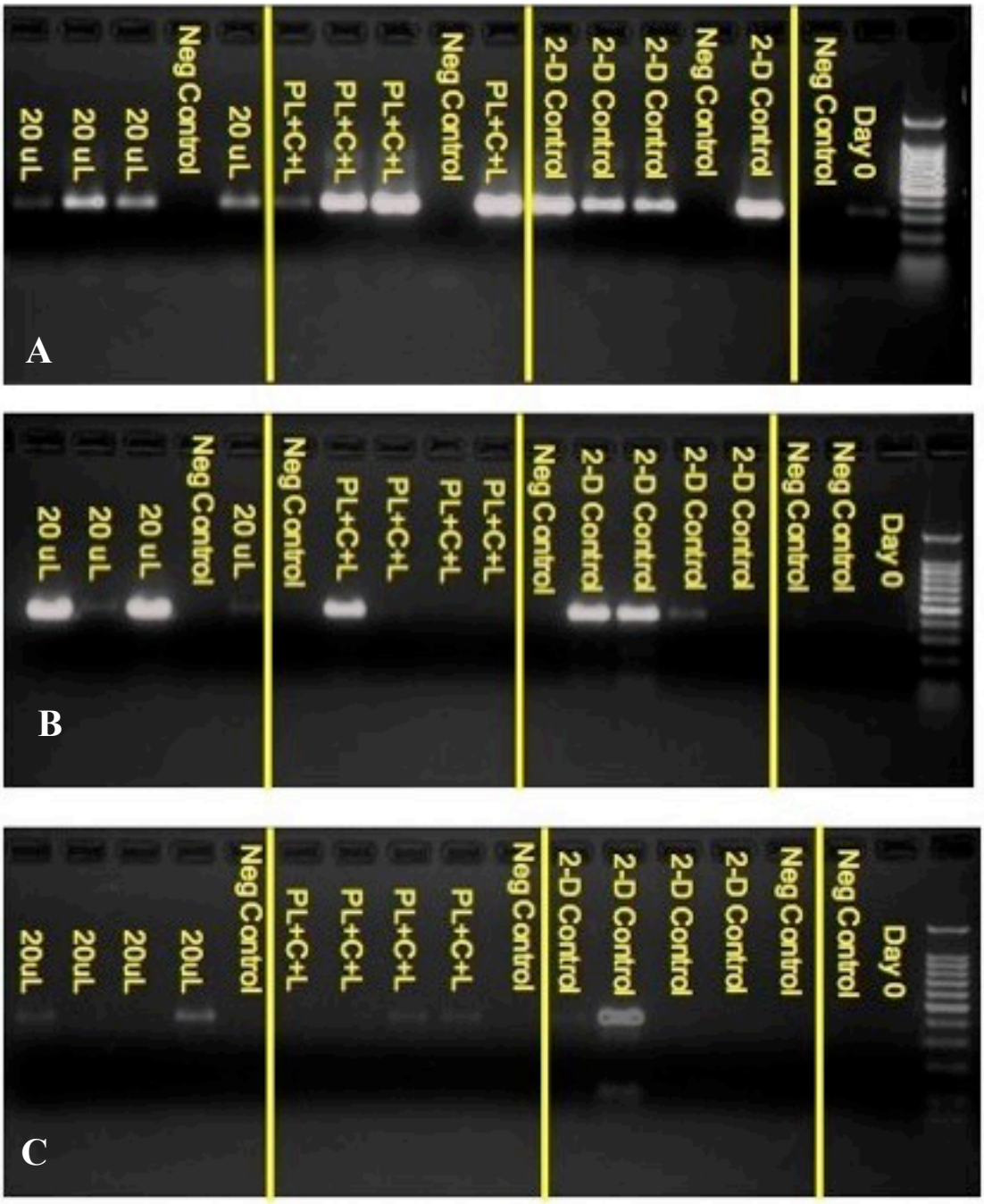

Figure 1.17 Gel electrophoresis results for cells seeded on negative controls, PL+C+L scaffolds, and positive controls for (A) Beta-Actin, (B) GADD 153, and (C) aP-2

DISCUSSION

The main objective of this research was to design 3-D polymer scaffolds that are viable for preadipocyte growth and differentiation and to assess the behavior and gene expression of cells grown on these scaffolds. Polylactide, a synthetic polymer, was used to fabricate control scaffolds to compare with polylactide scaffolds coated with collagen or collagen and linoleic acid. Each of these scaffolds was tested to determine its potential in an injectable composite for breast tissue engineering.

Polylactide beads were fashioned and used as the base for each type of scaffold created in this study. As an unmodified microsphere, polylactide has a smooth, hydrophobic surface. Cells have a low affinity to polylactide; to increase its cellular affinity, it is desirable to modify the polylactide to a more desirable configuration by altering the macroscopic structure or the surface characteristics. In order for 3-D polylactide scaffolds to have the potential to induce new adipose tissue formation, it will be necessary for these microspheres to support preadipocyte cell attachment.

Collagen was chosen as the surface coating material for polylactide because of its biodegradable and nontoxic properties. It is hydrophilic and, because it is a natural material, has cell recognition sites that facilitate cellular attachment. Linoleic acid was coated onto a set of beads with collagen to encourage preadipocyte differentiation and, eventually, adipocyte lipid filling.

Initially, collagen was added to a solution of polylactide before being made into beads. Beads from this mixture were almost 13 times smaller than PL beads. Fibroblasts were shown to have a high affinity to these collagen encapsulated PL beads, shown by

the larger number of cells attached to these scaffolds than the PL microspheres and the continual cellular proliferation on the collagen encapsulated beads. Collagen inside the beads could have increased cell affinity once released from the bead, due to the collagen's compatible chemistry, although collagen was not conclusively proven to be present by Gomori's One Step Trichrome or FTIR. The dramatic difference in size caused by the addition of collagen is also a likely reason cells had a greater affinity for these beads [32, 33]. These beads also appear to contain bubbles (not shown), which may have affected the surface of the beads and therefore affected cell attachment and growth. Although one or more of these reasons could have affected cell affinity for these beads, the increased cellular affinity is most likely due to the smaller size of these beads.

Since collagen was not proven present in the previous beads, collagen was added to the polylactide using a different method. Hong and colleagues created a way to graft collagen to the surface of PL beads, thus ensuring collagen was present on the surface of the beads [34]. For one set of beads, linoleic acid was added to the solubilized collagen before coating. Both types of scaffolds were tested with preadipocytes.

In the final cell test, the scaffolds tested were PL beads, PL beads coated with collagen and PL beads coated with collagen and lipid. The coating of the scaffold influenced cellular attachment and behavior as showed from the LIVE/DEAD® assay, triglyceride assay, gas chromatography, RT-PCR, and lactic acid/glucose measurements. The preadipocytes cultured on both types of coated PL scaffolds attached to the scaffolds at an early time point, proliferated, and maintained or increased in total fatty acid content and triglyceride concentration throughout the entire study. The preadipocytes cultured on

the uncoated PL scaffolds had a later time point for attachment, and either maintained or decreased in total fatty acid content and triglyceride concentration; only a few scaffolds supported cell attachment.

The metabolic activity of the cells was determined by the lactic acid/glucose assay. Glucose, supplied in the medium, is the "food" for the cells and decreases in glucose concentration in the medium indicate an increase in overall metabolic activity. Medium from all of the scaffolds continually decreased in glucose concentration from the second Day of the study to the last Day of the study. Lactic acid is waste produced by active cells and increases in lactic acid concentration in the medium indicate overall metabolic activity. In all scaffolds except PL beads and PL+C+L, beads lactic acid concentration increased between Day 4 and Day 18. All scaffolds increased in lactic acid production between Day 10 and Day 18.

These results suggest that the cells are proliferating on the all of the scaffolds. Lactic acid results for cells cultured on PL and PL+C+L beads show there was possibly a delay in significant cell growth until Day 10, although glucose consumption had increased since the beginning of the culture. For the PL scaffolds, this delay in significant lactic acid production is due to the fact that cells have a low affinity for the surface of the beads so have a harder time attaching and then dividing.

Interestingly, all scaffolds significantly decreased in lactic acid concentration from Day 4 to Day 6 and all scaffolds except for PL and PL+C+L increased significantly from Day 2 to Day 4. The increase on Day 4 is because the cells that attached on Day 2 are dividing. There was no increase for cells cultured on PL beads; far fewer cells

attached to these relatively hydrophobic scaffolds and these cells probably did not divide immediately. The introduction of the linoleic acid may have disturbed the natural progression of cellular attachment and division. Cells could attach to the beads, but once there, many of the cells may have focused on remodeling the linoleic acid before dividing, which would explain why there is a non-significant increase.

LIVE/DEAD images for the 3-D scaffolds show quantitatively that cells grown on all of the scaffolds increased in number during the culture period, but at different rates. Cells grown on PL beads took the longest to start growing on the beads and the fewest cells visible. It was not until Day 10 that any cells were seen growing on the PL beads and at Day 18, only a few beads were partially covered with cells. For cells grown on both PL+C and PL+C+L beads, cells had already attached to the beads by Day 4, qualitatively increasing in cell number at each time point. By Day 18, most of the beads of both material types were almost completely covered. For all bead groups, beads without live cell attachment also did not have dead cell attachment, indicating that cells never attached to these beads.

It was expected that a larger number of cells would attach to the coated beads due to the presence of collagen. Research by von Heimburg and coworkers showed the affinity of preadipocytes to collagen scaffolds and that the cells also differentiated into mature adipocytes on the collagen scaffolds [35]. It was easier for the cells to attach to the collagen than the PL surface because the collagen is a natural, hydrophilic, nonantigenic material and it is recognizable to the cells. Both types of coated beads

facilitated improved cell attachment and cell proliferation rate as compared with the plain PL beads.

The triglyceride and total fatty acid assays measured production of triglyceride and fatty acid, both of which are produced by maturing preadipocytes and adipocytes. Triglycerides are composed of a glycerol and three fatty acids. The triglyceride assay measures glycerol concentration while gas chromatography breaks down all complex fatty acids to measure each fatty acid individually. The results from the triglyceride assay should correlate with the results from the gas chromatography assay. Increases in either could be due to an increase in cell number or due to an increase in cell productivity. Some of the triglyceride groups had a large standard deviation due to inconsistent cell growth between the different samples in each group.

Cells grown on the negative control 2-D surfaces did not display an increase in triglyceride or total fatty acid content, but did display a significant increase in linoleic acid from Day 4 to Day 18. The cells cannot produce linoleic acid, so any linoleic acid in the cells must be extracted from the medium or scaffolds and then incorporated into the cells. This increase indicates that linoleic acid was present in the medium and that the cells were incorporating fatty acids. Images taken of these cells showed that most cells still maintained fibroblast-like morphologies on Day 18, but that some had developed rounded morphologies. Fischbach and coworkers showed that preadipocytes did not differentiate in culture without differentiation inducers [36]. Cells cultured on the positive control scaffolds increased in total fatty acid content between Days 10 and 18 and specifically increased in linoleic acid between Days 4 and 10. Images on Day 10

showed some cells with rounded morphology and, by Day 18, some cells with lipid droplets present. The addition of linoleic acid to the medium, with no other differentiation inducers, facilitated a quicker transition from a fibroblast-like state to a round, lipid filled state.

The cells cultured on the 3-D scaffolds developed more slowly than the cells cultured on the 2-D scaffolds. Cells cultured on PL beads had constant triglyceride production and a decrease in total fatty acid content over the entire culture period. Since the lactic acid/glucose measurements indicate that cell numbers increased between Days 10 and 18, the cells created less triglycerides and fatty acids as time progressed. Samples from both PL+C and PL+C+L scaffolds increased in triglyceride but not in total fatty acid. This occurrence is most likely due to an increase in the number of cells as time progressed, as indicated by the lactic acid/glucose measurements. The results from the triglyceride assay and total fatty acid assay should show similar trends for each of the samples, but there were significant differences between the results derived from the two assays. This difference is most likely due to the fact that the procedure for gas chromatography has not been optimized for cells grown on polymer beads.

Only two individual cultures, of all the 3-D scaffolds samples, had linoleic acid present and it was only present on Day 10. These samples were not extracted from the cells cultured on the PL+C+L beads, so the linoleic acid was not from the initial coating of the beads. The linoleic acid was not present in other cultures from the same group and sample day, and was not present in previous or later days. This result therefore is most

likely an artifact due to from insufficient rinsing of these two samples on that particular day, rather than as a result of cells incorporating the linoleic acid.

RT-PCR was used to analyze gene expression of specific preadipocyte and mature adipocyte genes. The expression of these genes helps to determine the extent of cell differentiation. Gene expression was analyzed for cells cultured on the control 2-D scaffolds, cells cultured on 2-D scaffolds with 20 μL of linoleic acid, and cells cultured on PL+C+L scaffolds. An RIN of less than 8 is not viable for further testing. Cells cultured on PL beads and PL+C beads were extremely low in number and therefore did not have enough viable RNA to test for gene expression.

The primers for β-actin, GADD 153, PPAR-γ, and aP-2 were designed by Nichole Cavin, though the optimal primer conditions were different than previously recorded [37]. PPAR-γ was not detected in any sample. This is most likely due to incorrectly designed primers or conditions for the assay were not properly optimized for this primer. The cells grown on the control 2-D scaffold expressed GADD 153 in three of the four samples, and one of those samples also strongly expressed aP-2. All four of the samples of cells supplemented with 20 μL linoleic acid expressed GADD 153; two of those samples expressed it very strongly. Two of the cultures expressed aP-2 weakly. These results indicate that both 2-D scaffolds had cell populations consisting of preadipocytes and mature adipocytes. Only one sample of cells grown on PL+C+L beads expressed GADD 153, while two different samples grown on these beads expressed aP-2 weakly.

GADD 153 is a growth arrest gene that is expressed during a cell's exit from the growth cycle and entry into differentiation. It has been reported that GADD 153 is

expressed during growth arrest in preadipocytes, then down regulated as the preadipocytes enter the differentiation cycle [38]. However, Darlington and coworkers report that GADD 153 is expressed at low levels in confluent preadipocytes and is suppressed throughout clonal expansion before adipogenesis [39]. GADD 153 is elevated on Day 4 of differentiation and remains elevated throughout differentiation [39]. Literature reports do agree that GADD 153 is not expressed until cells become confluent. The expression of GADD 153 in the results published here indicate that the cells from all three scaffold types tested are, at the very least, entering the differentiation stage by undergoing growth arrest, which is the first stage of differentiation.

Two cells populations grown on the control 2-D scaffold and two cell populations grown on the 2-D scaffolds with 20uL linoleic acid supplement expressed both GADD 153 and aP-2. Since aP-2 is only expressed in mature adipocytes, these results indicate that the cell populations of these scaffolds are a heterogeneous mix of preadipocytes and mature adipocytes. Two populations of cells grown on PL+C+L beads expressed aP-2 but did not express GADD 153, although one other population of cells grown on PL+C+L did express GADD 153. This result indicates that cells grown on these scaffolds are also a heterogeneous mix of preadipocytes and mature adipocytes.

Since there are conflicting reports regarding the timing of GADD 153 expression during preadipocyte differentiation, and without knowing the expression profile for PPAR-γ, it is difficult to know why some cell populations are not expressing GADD 153 at all. The samples that contain no GADD 153 could either be preadipocytes before

growth arrest, preadipocytes undergoing clonal expansion, or preadipocytes undergoing differentiation, depending on which previous research is to be believed.

Even though cells could attach to all of the microspheres, regardless of the surface chemistry, the cell numbers are different when comparing those cultivated on PL surfaces and those cultivated on collagen PL surfaces. The addition of collagen to the surface of the beads significantly increased the cell attachment rate and possible growth rate. Relatively more cells were observed on the beads with collagen and with collagen and linoleic acid surfaces than on the PL beads. The collagen presented a compatible surface for the cells to recognize and bind to.

The effect of adding linoleic acid to the surface of the beads was not clearly determined. McNeel and coworkers found that the effect of linoleic acid on preadipocytes was the same no matter the type of isomer [40]. This is why linoleic acid and not conjugated linoleic acid was tested on these beads. However, Satory and Smith reported that conjugated linoleic acid inhibits preadipocyte proliferation and promotes lipid filling of these cells over a range of concentrations [30]. Also, since conjugated linoleic acid is composed of positional and geometric isomers of linoleic acid, the type of linoleic acid may have different effects on preadipocytes [41, 42]. The reason we did not see any significant differences between the beads coated with collagen and the beads coated with collagen and linoleic acid is likely due to the concentration of linoleic acid on the surface of the beads. One linoleic acid concentration was chosen in order to simply determine if linoleic acid could be added to the surface of the beads.

The DSC results indicate that the original polymer used to construct the PL scaffolds is semi-crystalline. There were no DSC-induced crystallization peaks but a melting peak was present. The polylactide microsphere fabrication process did not affect the crystallinity of the polymer.

The fabrication of the PL beads did decrease the molecular weight of the polymer. The creation of the PL beads likely cleaves the larger molecular weight chains, causing a decrease in overall weight average molecular weight. The polydispersity of a polymer is the ratio of weight average molecular weight to the number average molecular weight, and is an indication of the distribution of molecular weights within the polymer. There was no significant difference between the as-received PL and the PL beads indicating that fabrication of the beads did not affect distribution of the molecular weights.

The scaffolds selected were tested with the goal of eventual use in an injectable composite system. The composite system may include different types of beads that will serve specific purposes. Collagen and linoleic acid coated beads could serve as cell attachment sites, while PL beads could serve another purpose other than cellular interaction. The fabrication and degradation of PL., as well as the cellular and tissue reaction to PL have been well documented by many researchers [18, 43]. PL could serve many functions in a composite system, such as a bulking agent, a mechanical support device, or a delivery system for growth factors, differentiation components, or therapeutic drugs.

CONCLUSIONS

In the initial study, collagen was encapsulated in polylactide beads, which caused the beads to be 13 times smaller than polylactide beads. These beads were cultured with fibroblasts in stir flasks and tested for cellular viability. Cells cultured with the collagen encapsulated beads attached to the beads and proliferated on them through out the entire culture period, while cells cultured with the polylactide beads did not attach to the beads but aggregated together instead. Collagen was not proven to be present in the beads and therefore were not tested further.

Two types of coated polylactide beads were created and tested in a cell culture of preadipocytes. Coating the polylactide affected cellular attachment, cellular proliferation, and triglyceride and fatty acid production. The collagen coating increased cellular attachment, proliferation, and triglyceride production of the preadipocytes compared to that resulting from culture with uncoated polylactide beads. The concentration of linoleic acid in the coating did not have a measurable affect on cellular activity, but linoleic acid added to medium on a 2-D plate increased fatty acid production in preadipocytes. Collagen coated beads show promise to be used in a tunable system as cellular carriers and for the promotion of cellular growth. Coated and uncoated scaffolds can be used in combination to form an injectable composite system, the coated beads functioning as a cellular carrier and the uncoated beads serving as a drug delivery or tissue bulking device.

RECOMMENDATIONS

Future studies should research an optimal concentration of linoleic acid for inducing differentiation in preadipocytes.

Studies should research coating different concentrations of linoleic acid on the surface of microspheres.

Further studies should research the effects of differing concentrations of tannic acid on collagen and linoleic acid content in the surface coating.

Other types of fatty acid should be researched as a coating for microspheres.

Real time RT-PCR and more preadipocyte and adipocyte specific genes should be used to evaluate the gene expression.

More research should go into optimizing the gas chromatography procedure for polymer beads.

A co-culture of preadipocytes with other cells found in the breast should be researched further.

Further studies should determine an appropriate hydrogel carrier for the injectable beads.

Future studies should be designed to test the effects of shear forces from injection on the integrity of the collagen coating.

APPENDICES

APPENDIX A

Triglyceride Assay (3 plates: day 4, day 10, day 18)

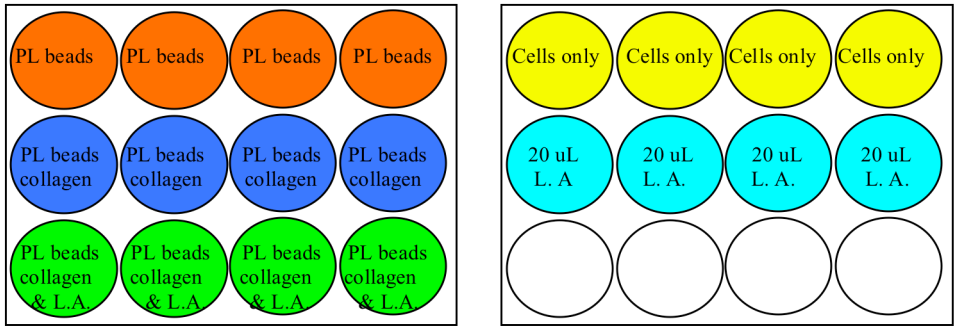

Total Fatty Acid Content Assay Assay (3 plates: day 4, day 10, day 18)

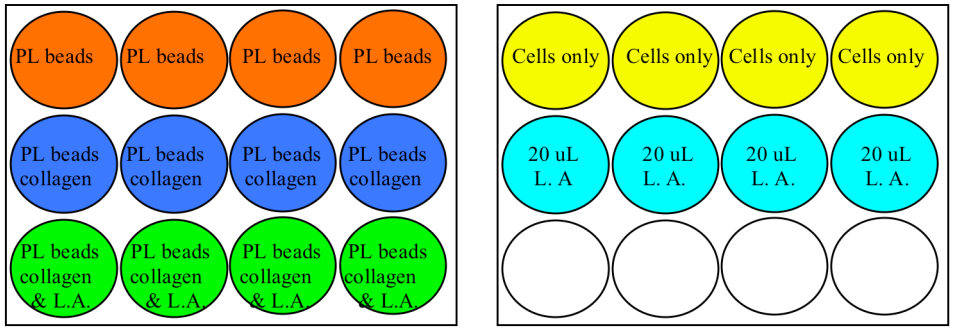

RT-PCR (1 plate: day 18)

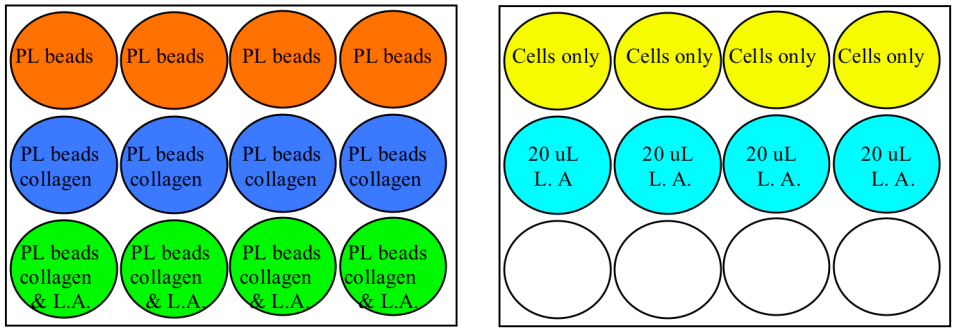

Orange: PL beads **Dark Blue:** Collagen coated PL beads **Green:** Collagen and Linoleic Acid (L.A.) coated PL beads **Yellow:** Cells on polystyrene **Light Blue:** Cells cultured with 20uL Linoleic acid (L.A.) on polystyrene

Figure A-1: 12-well plate layout for assessment of cellular activity and differentiation on 2-D versus 3-D scaffolds

LITERATURE CITED

1. American Cancer Society. *Cancer Facts and Figures 2007*. 2007 http://www.cancer.org.

2. Gregoire, F.M., C.M. Smas, and H.S. Sul, "Understanding adipocyte differentiation". Physiological reviews, 1998. **78**(3): p. 783-809.

3. Burton, G.R., Y. Guan, R. Nagarajan, and R.E. McGehee, Jr., "Microarray analysis of gene expression during early adipocyte differentiation". Gene, 2002. **293**(1-2): p. 21-31.

4. Gerhold, D.L., F. Liu, G. Jiang, Z. Li, J. Xu, M. Lu, J.R. Sachs, A. Bagchi, A. Fridman, D.J. Holder, T.W. Doebber, J. Berger, A. Elbrecht, D.E. Moller, and B.B. Zhang, "Gene expression profile of adipocyte differentiation and its regulation by peroxisome proliferator-activated receptor-gamma agonists". Endocrinology, 2002. **143**(6): p. 2106-2118.

5. Wright, H.M., C.B. Clish, T. Mikami, S. Hauser, K. Yanagi, R. Hiramatsu, C.N. Serhan, and B.M. Spiegelman, "A synthetic antagonist for the peroxisome proliferator-activated receptor gamma inhibits adipocyte differentiation". The Journal of biological chemistry, 2000. **275**(3): p. 1873-1877.

6. Wu, Z., N.L. Bucher, and S.R. Farmer, "Induction of peroxisome proliferator-activated receptor gamma during the conversion of 3T3 fibroblasts into adipocytes is mediated by C/EBPbeta, C/EBPdelta, and glucocorticoids". Molecular and cellular biology, 1996. **16**(8): p. 4128-4136.

7. Tamori, Y., J. Masugi, N. Nishino, and M. Kasuga, "Role of peroxisome proliferator-activated receptor-gamma in maintenance of the characteristics of mature 3T3-L1 adipocytes". Diabetes, 2002. **51**(7): p. 2045-2055.

8. Cowherd, R.M., R.E. Lyle, and R.E. McGehee, Jr., "Molecular regulation of adipocyte differentiation". Seminars in cell & developmental biology, 1999. **10**(1): p. 3-10.

9. Boney, C.M., P.A. Gruppuso, R.A. Faris, and A.R. Frackelton, Jr., "The critical role of Shc in insulin-like growth factor-I-mediated mitogenesis and differentiation in 3T3-L1 preadipocytes". Molecular endocrinology (Baltimore, Md, 2000. **14**(6): p. 805-813.

10. American Society of Plastic Surgeons. *2004 Reconstructive Surgery Procedures*. 2005

11. Lee, C.N. and R.D. Foster, "Breast reconstruction after mastectomy in young women". Breast disease, 2005. **23**: p. 47-52.

12. Patrick, C.W., "Breast tissue engineering". Annual review of biomedical engineering, 2004. **6**: p. 109-130.

13. Granzow, J.W., J.L. Levine, E.S. Chiu, and R.J. Allen, "Breast reconstruction with the deep inferior epigastric perforator flap: history and an update on current technique". J Plast Reconstr Aesthet Surg, 2006. **59**(6): p. 571-579.

14. Skalak, R. and C.F. Fox, *Tissue Engineering: proceedings of a workshop, held at Granlibakken, Lake Tahoe, California, February 26-29, 1998*. 1998, Liss: New York. p. 343.

15. Gomillion, C.T. and K.J. Burg, "Stem cells and adipose tissue engineering". Biomaterials, 2006. **27**(36): p. 6052-6063.

16. Chen, G., T. Ushida, and T. Tateishi, "Scaffold Design for Tissue Engineering." Macromol. Biosci., 2002. **2**(2): p. 67-75.

17. Bonassar, L.J. and C.A. Vacanti, "Tissue engineering: the first decade and beyond." J Cell Biochem Suppl, 1998. **30-31**: p. 297-303.

18. Griffith, L.G., "Emerging design principles in biomaterials and scaffolds for tissue engineering." Ann. N. Y. Acad. Sci., 2002. **961**: p. 83-95.

19. Patrick, C.W., Jr., "Tissue engineering strategies for adipose tissue repair." Anat Rec, 2001. **263**(4): p. 361-366.

20. Vacanti, J.P. and R. Langer, "Tissue engineering: the design and fabrication of living replacement devices for surgical reconstruction and transplantation." Lancet, 1999. **354 Suppl 1**: p. SI32-SI34.

21. Griffith, L.G. and G. Naughton, "Tissue engineering--current challenges and expanding opportunities." Science, 2002. **295**(5557): p. 1009-1014.

22. Nair, L.S. and C.T. Laurencin, "Polymers as biomaterials for tissue engineering and controlled drug delivery." Adv Biochem Eng Biotechnol, 2006. **102**: p. 47-90.

23. Sahoo, S.K., A.K. Panda, and V. Labhasetwar, "Characterization of porous PLGA/PLA microparticles as a scaffold for three dimensional growth of breast cancer cells." Biomacromolecules, 2005. **6**(2): p. 1132-1139.

24. Simon, C.G., Jr., N. Eidelman, S. B. Kennedy, A. Sehgal, C. A. Khatri, N. R. Washburn, "Combinatorial screening of cell proliferation on poly(L-lactic acid)/poly(D,L-lactic acid) blends." Biomaterials, 2005. **26**(34): p. 6906-6915.

25. Conejero, J.A., J. A. Lee, B. M. Parrett, M. Terry, K. Wear-Maggitti, R. T. Grant, A. S. Breitbart, "Repair of palatal bone defects using osteogenically differentiated fat-derived stem cells." Plast Reconstr Surg, 2006. **117**(3): p. 857-863.

26. Charulatha, V. and A. Rajaram, "Influence of different crosslinking treatments on the physical properties of collagen membranes." Biomaterials, 2003. **24**(5): p. 759-767.

27. Friess, W., "Collagen--biomaterial for drug delivery." Eur J Pharm Biopharm, 1998. **45**(2): p. 113-136.

28. Chung, K.T., T. Y. Wong, C. I. Wei, Y. W. Huang, Y. Lin, "Tannins and human health: a review." Crit Rev Food Sci Nutr, 1998. **38**(6): p. 421-464.

29. Burg, K.J. and T. Boland, "Minimally invasive tissue engineering composites and cell printing." IEEE Eng Med Biol Mag, 2003. **22**(5): p. 84-91.

30. Satory, D.L. and S.B. Smith, "Conjugated linoleic acid inhibits proliferation but stimulates lipid filling of murine 3T3-L1 preadipocytes." J Nutr, 1999. **129**(1): p. 92-97.

31. Ip, C., J.A. Scimeca, and H.J. Thompson, "Conjugated linoleic acid. A powerful anticarcinogen from animal fat sources". Cancer, 1994. **74**(3 Suppl): p. 1050-1054.

32. Malda, J. and C.G. Frondoza, "Microcarriers in the engineering of cartilage and bone". Trends Biotechnol, 2006. **24**(7): p. 299-304.

33. Maroudas, N.G., "Anchorage dependence: correlation between amount of growth and diameter of bead, for single cells grown on individual glass beads". Exp Cell Res, 1972. **74**(2): p. 337-42.

34. Hong, Y., C. Gao, Y. Xie, Y. Gong and J. Shen. "Collagen-coated polylactide microspheres as chondrocyte microcarriers." Biomaterials 2005. **26**(32): 6305-6313.

35. von Heimburg, D., S. Zachariah, I. Heschel, H. Kuhling, H. Schoof, B. Hafemann and N. Pallua, "Human preadipocytes seeded on freeze-dried collagen scaffolds investigated in vitro and in vivo." Biomaterials 2001. **22**: 429-438.

36. Fischbach, C., J. Seufert, H. Staiger, M. Hacker, M. Neubauer, A. Gopferich and T. Blunk, "Three-dimensional *in vitro* model of adipogenesis: comparison of culture conditions." Tissue Eng 2004 **10**(1/2): 215-229.

37. Cavin, A. N. M., *Adipocyte response to injectable breast tissue engineering scaffolds*. Department of Bioengineering. 2005. Clemson University: Clemson. **M. S.:** 119.

38. Tang, Q. Q. and M. D. Lane, "Role of C/EBP homologous protein (CHOP-10) in the programmed activation of CCAAT/enhancer binding protein-B during adipogenesis." Proc Natl Acad Sci U S A 2000. **97**: 12446-12450.

39. Darlington, G. J., S. E. Ross and O. A. MacDougald. "The role of C/EBP genes in adipocyte differentiation." J Biol Chem, 1998. **273**(46): 30057-30060.

40. McNeel, R.L., E.O. Smith, and H.J. Mersmann, "Isomers of conjugated linoleic acid modulate human preadipocyte differentiation". In Vitro Cell Dev Biol Anim, 2003. **39**(8-9): p. 375-382.

41. Brown, J. M. and M. K. McIntosh. "Conjugated linoleic acid in humans: regulation of adiposity and insulin sensitivity." J Nutr, 2003. **133**(10): 3041-3046.

42. Brown, J. M., Y. D. Halvorsen, Y. R. Lea-Currie, C. Geigerman and M. K. McIntosh. "Trans-10, cis 12, but not cis-9, trans-11, conjugated linoleic acid attenuates lipogenesis in primary cultures of stromal vascular cells from human adipose tissue." J Nutr, 2001. **131**: 2316-2321.

43. Simamora, P. and W. Chern. "Poly-L-lactic acid: an overview." J Drugs Dermatol, 2006. **5**(5): 436-440.